The Dissertation Committee for Allison Leigh Hall Certifies that this is the approved version of the following dissertation:

Understanding Changes in Post-Stroke Walking Ability through Simulation and Experimental Analyses

Committee:

Richard R. Neptune, Supervisor

Ronald E. Barr

Richard H. Crawford

Jonathan B. Dingwell

Steven A. Kautz

Understanding Changes in Post-Stroke Walking Ability through Simulation and Experimental Analyses

by

Allison Leigh Hall, B.S.; M.S.E.

Dissertation

Presented to the Faculty of the Graduate School of

The University of Texas at Austin

in Partial Fulfillment

of the Requirements

for the Degree of

Doctor of Philosophy

The University of Texas at Austin

December 2010

Dedication

I would like to dedicate this dissertation to my family for their love, support and encouragement throughout my life.

Acknowledgements

I would like to thank Dr. Rick Neptune, my advisor, for his guidance and wisdom which has made my graduate career a valuable experience and shaped me into the researcher I am today. I am grateful for the opportunities he has provided me to grow not only inside the lab, but outside the lab and for the challenging and interesting research I have been able to participate in throughout my time in graduate school. I would like to thank Dr. Steve Kautz for his insightful opinions and support of my research. I would also like to thank Dr. Ronald Barr, Dr. Richard Crawford and Dr. Jonathan Dingwell for serving on my dissertation committee.

I am extremely grateful for the past and present members of the Neuromuscular Biomechanics Lab who have provided important insight into my research and have become not only great collaborators, but great friends. I would also like to thank our collaborators at the University of Florida and the Malcom Randall VA Medical Center for their assistance with data collection and processing. I would also like to acknowledge Dr. Catherine Ambrose for introducing me to biomechanics research and motivating me to pursue graduate school.

Finally, I would like to thank my family and friends for providing me with unconditional support throughout my life. In particular, I would like to thank Kyle Kinney for keeping me laughing and for pushing me when I need to be pushed.

Understanding Changes in Post-Stroke Walking Ability through Simulation and Experimental Analyses

Publication No._____

Allison Leigh Hall, Ph.D.

The University of Texas at Austin, 2010

Supervisor: Richard R. Neptune

Post-stroke hemiparesis usually leads to slow and asymmetric gait. Improving walking ability, specifically walking speed, is a common goal post-stroke. To develop effective post-stroke rehabilitation interventions, the underlying mechanisms that lead to changes in walking ability need to be fully understood. The overall goal of this research was to investigate the deficits that limit hemiparetic walking ability and understand the influence of post-stroke rehabilitation on walking ability in persons with post-stroke hemiparesis.

Forward dynamics walking simulations of hemiparetic subjects (and speed-matched controls) with different levels of functional walking status were developed to investigate the relationships between individual muscle contributions to pre-swing forward propulsion, swing initiation and power generation subtasks and functional walking status. The analyses showed that muscle contributions to the walking subtasks are indeed related to functional walking status in the hemiparetic subjects. Increased contributions from the paretic leg muscles (i.e., plantarflexors and hip flexors) and

reduced contributions from the non-paretic leg muscles (i.e., knee and hip extensors) to the walking subtasks were critical in obtaining higher functional walking status.

Changes in individual muscle contributions to propulsion during rehabilitation were investigated by developing a large number of subject-specific forward dynamics simulations of hemiparetic subjects (with different levels of pre-training propulsion symmetry) walking pre- and post-locomotor training. Subjects with low paretic leg propulsion pre-training increased contributions to propulsion from both paretic leg (i.e., gastrocnemius) and non-paretic leg muscles (i.e., hamstrings) to improve walking speed during rehabilitation. Subjects with high paretic leg propulsion pre-training improved walking speed by increasing contributions to propulsion from the paretic leg ankle plantarflexors (i.e., soleus and gastrocnemius). This study revealed two primary strategies that hemiparetic subjects use to increase walking speed during rehabilitation.

Experimental analyses were used to determine post-training biomechanical predictors of successful post-stroke rehabilitation, defined as performance over a 6-month follow-up period following rehabilitation. The strongest predictor of success was step length symmetry. Other potential predictors of success were identified including increased paretic leg hip flexor output in late paretic leg single-limb stance, increased paretic leg knee extensor output from mid to late paretic leg stance and increased paretic leg propulsion during pre-swing.

Table of Contents

List of Tables

List of Figures

Chapter 1: Introduction

Stroke is the leading cause of long-term disability in the United States (Lloyd-Jones et al., 2010). Post-stroke hemiparesis is seen in 50% of persons six months following stroke (Kelly-Hayes et al., 2003) and is usually characterized by slow walking speed and asymmetry between the paretic and non-paretic legs (e.g., Olney and Richards, 1996). Walking speed is commonly used to predict stroke severity and assess functional walking status (i.e., household, limited community and community walking status) post-stroke (Bowden et al., 2008; Perry et al., 1995). Given that improving walking ability is a primary goal post-stroke (Bohannon et al., 1988; Harris and Eng, 2004), rehabilitation strategies are often focused on improving walking speed, and therefore walking status. Hemiparetic subjects typically have impaired muscle excitation (e.g., den Otter et al., 2007; Turns et al., 2007) and therefore altered muscle coordination (i.e., muscle force production and timing) that may limit walking speed. Properly graded muscle force and timing has been shown to be critical to achieving walking subtasks of body support, forward propulsion, leg swing initiation and power generation across walking speeds in healthy walking (e.g., Liu et al., 2008; Neptune et al., 2008).

Pre-swing (i.e., double support phase preceding toe-off) has been shown to be a critical phase of the gait cycle for performing these walking subtasks in healthy walking (e.g., Liu et al., 2008; Neptune et al., 2008) and several paretic leg pre-swing abnormalities, such as prolonged duration, reduced peak hip extension and reduced knee and hip flexion velocities, have been shown in hemiparetic walking (De Quervain et al., 1996). Therefore, it is likely that muscle contributions to the walking subtasks are altered during the pre-swing phase in hemiparetic walking. In order to develop more effective rehabilitation interventions, the underlying mechanisms that limit walking speed and, by

extension, lead to impaired functional walking status post-stroke need to be fully understood. In addition, understanding how post-stroke rehabilitation training changes muscle coordination will provide insight into the strategies that hemiparetic subjects use to improve walking speed.

Several experimental studies have examined post-stroke hemiparetic walking and identified factors that limit walking speed and therefore, if targeted during rehabilitation, have the potential to improve walking speed (Mulroy et al., 2010; Nadeau et al., 1999; Olney et al., 1991; Parvataneni et al., 2007; Teixeira-Salmela et al., 2001). However, these inverse dynamics-based studies have been limited due to their inability to quantify individual muscle contributions to segmental accelerations and power transfer between segments that are critical to understanding impaired muscle coordination in hemiparetic walking. Forward dynamics simulations have been used to quantify individual muscle contributions to walking subtasks in healthy walking (e.g., Liu et al., 2008; Neptune et al., 2008) and to body support in hemiparetic walking (Higginson et al., 2006), and therefore provide a powerful analysis tool for understanding how muscle coordination impacts walking ability in post-stroke hemiparetic subjects.

Therefore, the goal of the study in Chapter 2 was to use three-dimensional muscle-actuated forward dynamics simulations of hemiparetic subjects (and speed-matched controls) with different levels of functional walking status (i.e., limited community and community walkers) to investigate individual muscle contributions to pre-swing forward propulsion (i.e., forward acceleration of the pelvis), swing initiation (i.e., power delivery to the leg) and power generation (i.e., musculotendon power output) and identify changes in muscle coordination (i.e., muscle force production and timing) that reduce pre-swing deficits, increase walking speed and ultimately improve functional walking status in hemiparetic walking. In healthy walking, the ankle plantarflexors are

critical for accomplishing the walking subtasks of forward propulsion, swing initiation and power generation (Liu et al., 2008; McGowan et al., 2008; Neptune et al., 2001; Neptune et al., 2008). Previous studies have reported paretic leg ankle plantarflexor weakness in persons with post-stroke hemiparesis and have suggested that output from the paretic leg ankle plantarflexors is related to walking speed (Nadeau et al., 1999; Olney et al., 1991; Parvataneni et al., 2007). Therefore, it is expected that the paretic leg ankle plantarflexors, soleus and gastrocnemius, will have impaired contributions to the walking subtasks during pre-swing and that the contributions from these muscles will be related to functional walking status. The paretic leg hip flexors have been shown to compensate for reduced paretic leg ankle plantarflexor output in some hemiparetic subjects (Nadeau et al., 1999) and have been shown to provide swing initiation in healthy walking (Neptune et al., 2004; Neptune et al., 2008). Therefore, the contributions of the paretic leg hip flexors to swing initiation are also expected to be related to functional walking status in persons with post-stroke hemiparesis.

Post-stroke rehabilitation has been shown to be effective in improving walking speed in hemiparetic subjects (Ada et al., 2003; Barbeau and Visintin, 2003; Mulroy et al., 2010; Parvataneni et al., 2007; Peurala et al., 2005; Sullivan et al., 2007; Teixeira-Salmela et al., 2001; Visintin et al., 1998). However, improvements in walking speed can be achieved by a combination of increased paretic and non-paretic leg propulsion. Hemiparetic subjects have altered anterior-posterior ground reaction forces (AP GRFs) compared to healthy subjects (Bowden et al., 2006). However, it is not known how individual muscles contribute to the AP GRFs in hemiparetic walking or how the contributions change with improved walking speed following rehabilitation.

The goal of the study in Chapter 3 was to use three-dimensional muscle-actuated forward dynamics simulations of hemiparetic subjects walking pre- and post-locomotor

therapy intervention to investigate changes in individual muscle contributions to propulsion (i.e., anterior-posterior (AP) body center-of-mass (COM) acceleration) that lead to improved walking speed during rehabilitation. Previous studies of joint kinetics have shown that hemiparetic subjects increase power output from the paretic leg ankle plantarflexors in late stance (Mulroy et al., 2010; Parvataneni et al., 2007; Teixeira-Salmela et al., 2001) and the non-paretic leg hip extensors in early stance (Parvataneni et al., 2007; Teixeira-Salmela et al., 2001) following rehabilitation. Modeling and simulation studies have shown that the ankle plantarflexors (soleus and gastrocnemius) are the primary contributors to the AP GRFs in late stance and that the hamstrings contribute positively to the AP GRFs from early to mid-stance in healthy walking (Liu et al., 2008; Neptune et al., 2004). In addition, the knee and hip extensors can contribute positively to forward propulsion of the pelvis during foot-flat in healthy walking (Neptune et al., 2004). Therefore, it is expected that hemiparetic subjects may improve walking speed during rehabilitation by increasing contributions to propulsion from the paretic leg ankle plantarflexors and the non-paretic leg hip and knee extensors. Because of the heterogeneity of the hemiparetic population, it is expected that a variety of strategies exist to improve walking speed following rehabilitation. This study will develop a large number of simulations of hemiparetic walking to provide insight into the variability of the hemiparetic population and the strategies that hemiparetic subjects use to improve walking speed.

Previous studies have shown that after hemiparetic subjects complete rehabilitation training, most improvements in walking ability (as measured by self-selected walking speed) are maintained for three to six months (Barbeau and Visintin, 2003; Peurala et al., 2005; Sullivan et al., 2007; Visintin et al., 1998). However, no study has identified the biomechanical quantities that predict long-term success (as defined by

changes in self-selected walking speed over a 6-month follow-up period following training) in post-stroke rehabilitation. Quantities such as joint kinetics, step length, propulsion or daily step activity may be able to identify those subjects who will be successful following post-stroke rehabilitation. The results of this study will provide insight into the long-term effectiveness of rehabilitation training.

The goal of the study in Chapter 4 was to use experimental analyses of post-stroke hemiparetic subjects who completed a post-stroke rehabilitation training intervention to identify post-training biomechanical predictors of success (as measured by changes in self-selected walking speed over a 6-month follow-up period) following rehabilitation. Studies have shown that after rehabilitation, hemiparetic subjects increase paretic leg ankle plantarflexor and hip flexor joint power output with increased walking speed (Mulroy et al., 2010; Parvataneni et al., 2007; Teixeira-Salmela et al., 2001). In addition, the contribution of the paretic leg to the AP GRFs, step length asymmetry and daily step activity have been shown to be indicators of hemiparetic severity and self-selected walking speed (Balasubramanian et al., 2007; Bowden et al., 2006; Bowden et al., 2008). Therefore, it is expected that the paretic leg ankle plantarflexor moment impulse (i.e., time integral of the joint moment), the paretic leg hip flexor moment impulse, step length asymmetry, the paretic leg AP GRF impulse (i.e., time integral of the AP GRF) and daily step activity will be predictors of successful post-stroke rehabilitation, which will be defined as changes in self-selected walking speed over a 6-month follow-up period following training.

The overall goal of this research is to investigate the underlying mechanisms that influence functional walking ability in post-stroke hemiparetic walking and understand the impact of post-stroke rehabilitation on walking ability in persons with post-stroke hemiparesis. This research will combine modeling and simulation techniques and

experimental analyses to accomplish this goal. The results of this work will determine the relationships between muscle coordination and functional walking status in hemiparetic subjects and will reveal the changes in muscle coordination associated with improved functional walking status. This will be the first study to develop a large number of subject-specific forward dynamics simulations of post-stroke hemiparetic walking and will provide insight into the variability of the hemiparetic population. In addition, this study will reveal biomechanical predictors of successful post-stroke rehabilitation and the results will help to identify hemiparetic subjects who will continue to improve following rehabilitation. The results of this research will provide insight into the factors that limit mobility in the hemiparetic population and develop rationale for designing effective post-stroke rehabilitation strategies.

Chapter 2: Relationships between Muscle Contributions to Walking Subtasks and Functional Walking Status in Persons with Post-Stroke Hemiparesis

Introduction

Post-stroke hemiparesis is seen in 50% of persons six months following stroke (Kelly-Hayes et al., 2003) and is often characterized by slow walking speed and asymmetry between the paretic and non-paretic legs (e.g., Olney and Richards, 1996). Walking speed is commonly used to predict stroke severity and assess functional walking status (i.e., household, limited community and community walking status) post-stroke (Bowden et al., 2008; Perry et al., 1995). Given that improving walking ability is a primary goal post-stroke (Bohannon et al., 1988), rehabilitation strategies focused on improving walking speed, and therefore functional walking status, are important. In order to develop more effective rehabilitation interventions, the underlying mechanisms that lead to different levels of walking status need to be fully understood.

Previous studies have shown that the ankle plantarflexors, soleus (SOL) and gastrocnemius (GAS), are essential to the walking subtasks of forward propulsion (i.e., pelvis forward acceleration), swing initiation (i.e., power delivery to the leg) and power generation (i.e., musculotendon power output) in healthy walking and that pre-swing (i.e., double support phase preceding toe-off) is a critical region of the gait cycle for SOL and GAS to accomplish these subtasks (Liu et al., 2008; McGowan et al., 2008; Neptune et al., 2001; Neptune et al., 2008). SOL and GAS have unique contributions to the walking subtasks, with SOL contributing primarily to trunk forward propulsion while GAS contributes primarily to leg swing initiation (Neptune et al., 2001; Neptune et al., 2008). Plantarflexor weakness is commonly observed in hemiparetic walking and the output from the paretic plantarflexors has been correlated with walking speed (Nadeau et al.,

1999; Olney et al., 1991; Parvataneni et al., 2007). We have recently suggested that impaired performance in forward propulsion, swing initiation and power generation in hemiparetic subjects is at least partially due to decreased paretic plantarflexor contributions, specifically with reduced SOL contributions impairing forward propulsion, reduced GAS contributions impairing swing initiation and reduced SOL and GAS contributions impairing power generation (Nott et al., 2010; Peterson et al., 2010). However, the relationships between plantarflexor contributions to specific walking subtasks and functional walking status in hemiparetic walking are not known.

Studies of healthy adults have shown the uniarticular hip flexors, iliacus and psoas (IL), provide swing initiation together with GAS (Neptune et al., 2004; Neptune et al., 2008) and that IL can compensate for overall plantarflexor weakness in some hemiparetic subjects (Nadeau et al., 1999; Olney and Richards, 1996). However, we have shown through experimental and simulation studies that contributions of paretic IL to swing initiation and power generation are reduced in hemiparetic subjects relative to controls (Nott et al., 2010; Peterson et al., 2010). Thus, the relationship between paretic IL contributions to swing initiation and power generation and functional walking status in hemiparetic walking has not been established.

The goal of this study was to investigate differences in pre-swing forward propulsion, swing initiation and power generation among hemiparetic subjects (and speed-matched controls) with different levels of functional walking status (i.e., limited community and community walkers) using muscle-actuated forward dynamics simulations to identify changes in muscle coordination (i.e., muscle force production and timing) that reduce pre-swing deficits, increase walking speed and ultimately improve functional walking status in hemiparetic walking. Forward dynamics simulations provide an ideal framework to achieve this goal as they have been used to successfully quantify

individual muscle contributions to the walking subtasks in healthy walking (e.g., Liu et al., 2008; Neptune et al., 2008) and to body support in hemiparetic subjects (Higginson et al., 2006). We expect that decreased muscle contributions to the walking subtasks during the pre-swing phase limits the functional walking status of hemiparetic subjects, with subjects who perform better in the three subtasks attaining higher walking speeds and higher functional walking status than subjects who have more impaired performance in one or more of the subtasks. We expect that the contributions of the paretic leg ankle plantarflexors (SOL and GAS) and the uniarticular hip flexors (IL) to forward propulsion, swing initiation and power generation will be reduced in hemiparetic subjects relative to controls, with the difference increasing (representing more impairment) as functional walking status decreases. By identifying the walking subtasks and specific muscle groups that limit functional walking status in hemiparetic subjects, this study will provide insight into the underlying mechanisms that contribute to reduced performance in the hemiparetic subjects and provide rationale for developing effective post-stroke rehabilitation interventions.

Methods

Musculoskeletal Model

A previously described 3D musculoskeletal model (Peterson et al., 2010) (Appendix A: Fig. A2) with 23 degrees-of-freedom was used to generate forward dynamics walking simulations of control and hemiparetic subjects. The model was developed using SIMM (MusculoGraphics, Inc., Santa Rosa, CA, USA) and included rigid segments representing the trunk, pelvis and two legs (thigh, shank, talus, calcaneus and toes). The pelvis had 6 degrees-of-freedom (3 translations and 3 rotations) with

trunk and hip joints modeled by spherical joints. The knee, ankle, subtalar and metatarsophalangeal joints were modeled as single degree of freedom revolute joints. The foot-ground contact was modeled using 31 visco-elastic elements with coulomb friction attached to each foot (Neptune et al., 2000). Passive torques were applied at each joint to represent the forces applied by the ligaments, passive tissues and joint structures (Anderson, 1999; Davy and Audu, 1987). The dynamical equations of motion were generated using SD/FAST (PTC, Needham, MA, USA) and the forward dynamics simulations were produced using framework provided by Dynamics Pipeline (MusculoGraphics, Inc., Santa Rosa, CA, USA).

The musculoskeletal model was actuated with 43 individual Hill-type musculotendon actuators per leg (Table 2.1). The muscle excitation patterns were defined using a bimodal Henning pattern as:

$$e(t)=\sum_{i=1}^{2}\begin{cases}\frac{a_i}{2}\left[1-\cos\left(\frac{2\pi(t-onset_i)}{offset_i-onset_i}\right)\right], & onset_i\le t\le offset_i \\ 0, & \text{otherwise}\end{cases} \quad (2.1)$$

where $e(t)$ is the excitation magnitude at time t and a_i, $onset_i$ and $offset_i$ are the amplitude, onset and offset, respectively, of each mode, i. Musculotendon lengths and moment arms for each muscle were calculated using polynomial regression functions described by Menegaldo et al. (2004). Additional details about the polynomial regression functions are provided in Appendix A. The muscle contraction dynamics were governed by Hill-type muscle properties (Zajac, 1989) and the activation dynamics were modeled by a first-order differential equation (Raasch et al., 1997), with activation and deactivation time constants derived from Winters and Stark (1988). Nominal activation

and deactivation time constants of 12 and 48 ms, respectively, were used for muscles not available in Winters and Stark.

Table 2.1. The 43 musculotendon actuators per leg were combined into 18 groups after analysis according to anatomical classification and how they contributed to the three walking subtasks.

Muscle Name	Analysis Group
Iliacus	IL
Psoas	IL
Adductor Longus	AL
Adductor Brevis	AL
Pectineus	AL
Quadratus Femoris	QF
Superior Adductor Magnus	AM
Middle Adductor Magnus	AM
Inferior Adductor Magnus	AM
Sartorius	SAR
Rectus Femoris	RF
Vastus Medialis	VAS
Vastus Lateralis	VAS
Vastus Intermedius	VAS
Anterior Gluteus Medius	GMED
Middle Gluteus Medius	GMED
Posterior Gluteus Medius	GMED
Piriformis	PIRI
Gemellus	GEM
Anterior Gluteus Minimus	GMIN
Middle Gluteus Minimus	GMIN
Posterior Gluteus Minimus	GMIN
Tensor Fascia Lata	TFL
Anterior Gluteus Maximus	GMAX
Middle Gluteus Maximus	GMAX
Posterior Gluteus Maximus	GMAX
Semitendinosus	HAM
Semimembranosus	HAM
Gracilis	HAM
Biceps Femoris Long Head	HAM
Biceps Femoris Short Head	BFSH
Medial Gastrocnemius	GAS
Lateral Gastrocnemius	GAS
Soleus	SOL
Tibialis Posterior	SOL
Peroneus Brevis	SOL
Peroneus Longus	SOL
Flexor Digitorum Longus	SOL
Flexor Hallucis Longus	SOL
Tibialis Anterior	TA
Extensor Digitorum Longus	TA
Peroneus Tertius	TA
Extensor Hallucis Longus	TA

Dynamic Optimization

Forward dynamics simulations (from midstance to toe-off) were generated to emulate group-averaged experimentally measured kinematics and ground reaction forces (GRFs) of limited community and community hemiparetic subjects walking at their self-selected treadmill speed (limited community walkers: mean = 0.55 m/s (SD = 0.15 m/s); community walkers: mean = 0.92 m/s (SD = 0.05 m/s)) and elderly speed-matched control subjects walking at 0.6 and 0.9 m/s. The muscle excitation patterns (amplitude and timing) and the initial joint angular velocities were optimized using a simulated annealing algorithm (Goffe et al., 1994) that minimized differences between the simulated and experimental data (Appendix A: Fig. A1). Quantities included in the cost function were the 3D pelvis translations and rotations, 3D trunk rotations, hip, knee and ankle joint angles and 3D GRFs. Muscle stress was also minimized in the cost function to ensure an even distribution across muscle groups.

Experimental Data Collection

Experimental GRF, kinematic and electromyographic (EMG) data were collected as part of a larger data set (Nott et al., 2010) from 57 hemiparetic subjects (30 left hemiparesis; 37 men; age: mean = 61.4 years (SD = 11.4 years); time since stroke: mean = 5.0 years (SD = 5.5 years) and 21 elderly control subjects (4 men; age: mean = 65.2 years (SD = 9.6 years)). Each subject walked on an ADAL split-belt instrumented treadmill (Tecmachine, Andrézieux Bouthéon, France) while data were collected for 30 seconds (Appendix C). Hemiparetic subjects walked at their self-selected speed and elderly control subjects walked at their self-selected speed and at prescribed speeds of 0.3, 0.6 and 0.9 m/s. All subjects provided written informed consent approved by the Institutional Review Boards of the University of Florida and the University of Texas at

Austin. 3D GRF data were measured at 2000 Hz and low pass filtered at 20 Hz. Reflective marker trajectories were recorded at 100 Hz and low pass filtered at 6 Hz. Surface EMG data were recorded bilaterally at 2000 Hz from the tibialis anterior, medial gastrocnemius, soleus, rectus femoris, biceps femoris long head, vastus medialis, semimembranosus and gluteus medius using a 16-channel EMG system (Konigsburg Instruments, Pasadena, CA, USA). The raw EMG data were high-pass filtered at 40 Hz, demeaned, rectified and low-pass filtered at 4 Hz. All data were processed using Visual3D (C-motion, Inc., Germantown, MD, USA). All data were time normalized to the paretic (right) leg gait cycle for the hemiparetic (control) subjects and averaged across gait cycles within each subject for each condition. Data were averaged across hemiparetic subjects in each functional group (limited community (n = 21); community (n = 5)) and control subjects walking at prescribed speeds (0.6 m/s (n = 20); 0.9 m/s (n = 17)) to generate the tracking data for each optimization. Subject characteristics for the hemiparetic and control subjects are provided in Tables B1, B2 and B3 in Appendix B. The EMG data were used to constrain the timing (onset and offset) for each muscle excitation pattern in the optimization to ensure muscles were producing force at the appropriate point in the gait cycle.

Analysis of Muscle Function

Performance of the walking subtasks during the pre-swing phase was quantified by individual muscle contributions to forward propulsion, swing initiation and power generation. A muscle-induced acceleration and segment power analysis (Fregly and Zajac, 1996) was performed to quantify individual muscle contributions to the walking subtasks (e.g., Neptune et al., 2001; Neptune et al., 2004; Neptune et al., 2008). Each

muscle's contribution to forward propulsion was determined by quantifying its average contribution to the horizontal pelvis acceleration during pre-swing. Muscle-induced mechanical power generated, absorbed or transferred to or from each segment within the leg was summed and averaged over the pre-swing phase to determine each muscle's contribution to swing initiation. Power generation for each muscle was calculated as the average musculotendon power during pre-swing. Contributions from individual muscles were grouped after analysis according to anatomical classification and how they contributed to the walking subtasks (Table 2.1, Appendix A: Fig. A2). The contributions of the muscle groups to each of the waking subtasks were compared across the hemiparetic and control groups to identify the relationships between performance of the subtasks and functional walking status.

Results

The kinematic and GRF data from the control and hemiparetic simulations agreed well with the experimental data, with an average absolute difference of 5.0 degrees and 3.8% BW for all simulations (Table 2.2, Appendix D). The timing of the optimized excitation patterns generally agreed with the experimentally collected EMG data as in our previous work (e.g., Neptune et al., 2001; Neptune et al., 2004).

Table 2.2. The average difference between the experimental and simulated kinematic angles and ground reaction forces (GRFs) compared to the average standard deviation (SD) of the experimental data. For each quantity: the average difference (2 SD) is reported.

			Controls at 0.6 m/s	Controls at 0.9 m/s	Limited Community	Community
Kinematic Angles (degrees)	**Pelvis**	Obliquity	2.704 (3.946)	1.492 (3.768)	1.508 (7.692)	2.382 (4.270)
		Rotation	1.983 (7.545)	3.511 (7.553)	2.299 (13.513)	2.923 (9.923)
		Tilt	6.283 (13.480)	9.581 (12.736)	3.085 (13.154)	5.608 (12.813)
	Trunk	Obliquity	3.032 (5.510)	3.363 (4.895)	2.187 (8.496)	2.432 (8.572)
		Rotation	6.298 (11.807)	7.879 (11.212)	4.773 (9.720)	5.043 (12.567)
		Tilt	0.460 (15.423)	3.233 (16.324)	2.272 (13.822)	6.650 (16.666)
	Ipsilateral/ Paretic Leg	Hip Adduction	3.329 (5.214)	2.125 (5.899)	2.833 (9.470)	7.345 (8.901)
		Hip Rotation	8.411 (27.203)	5.185 (28.223)	8.873 (22.658)	16.894 (13.096)
		Hip Flexion	6.113 (18.516)	7.350 (17.729)	13.528 (21.992)	12.702 (18.188)
		Knee Flexion	4.512 (14.618)	4.268 (13.153)	14.228 (24.921)	5.156 (17.918)
		Ankle Dorsiflexion	3.169 (11.446)	6.648 (12.073)	3.857 (11.409)	9.831 (9.687)
	Contralateral/ Non-Paretic Leg	Hip Adduction	2.073 (8.987)	1.237 (7.879)	10.242 (12.738)	2.432 (11.952)
		Hip Rotation	11.392 (29.202)	4.810 (25.971)	1.643 (19.508)	2.455 (18.852)
		Hip Flexion	5.036 (15.275)	5.820 (15.378)	2.880 (21.553)	6.234 (22.461)
		Knee	8.367 (14.817)	2.465 (12.907)	4.538 (17.193)	2.921 (19.668)
		Ankle Dorsiflexion	2.291 (10.598)	2.434 (11.308)	1.744 (10.272)	6.109 (7.255)
Forces (%BW)	**Ipsilateral/ Paretic Leg**	Anterior-Posterior GRF	2.443 (5.129)	3.218 (5.507)	1.101 (3.684)	1.891 (4.931)
		Vertical GRF	6.961 (18.176)	12.663 (19.425)	6.120 (23.843)	10.930 (27.468)
		Medial-Lateral GRF	1.813 (2.717)	3.070 (2.780)	2.082 (2.577)	0.719 (1.677)
	Contralateral/ Non-Paretic Leg	Anterior-Posterior GRF	3.094 (4.514)	1.084 (4.770)	0.655 (4.526)	0.505 (4.552)
		Vertical GRF	7.560 (17.014)	7.661 (18.538)	8.691 (26.679)	4.378 (24.313)
		Medial-Lateral GRF	1.411 (3.164)	1.898 (3.344)	1.355 (2.971)	1.123 (3.278)
Average Angle Error (degrees)			**4.716**	**4.463**	**5.031**	**6.070**
Average GRF Error (%BW)			**3.880**	**4.932**	**3.334**	**3.258**

Forward Propulsion

In the control subjects, contributions to forward propulsion from the ipsilateral and contralateral leg muscles increased and decreased, respectively, with increased walking speed (Fig. 2.1: Total). Contributions from the ipsilateral and contralateral leg muscles to pelvis deceleration (negative values) were similar as walking speed increased (Fig. 2.1: Total).

In the hemiparetic subjects, contributions from the paretic and non-paretic leg muscles to forward propulsion increased and decreased, respectively, with improved functional walking status (Fig. 2.1: Total). Contributions from the paretic and non-paretic leg muscles to pelvis deceleration increased and decreased, respectively, as functional walking status improved (Fig. 2.1: Total).

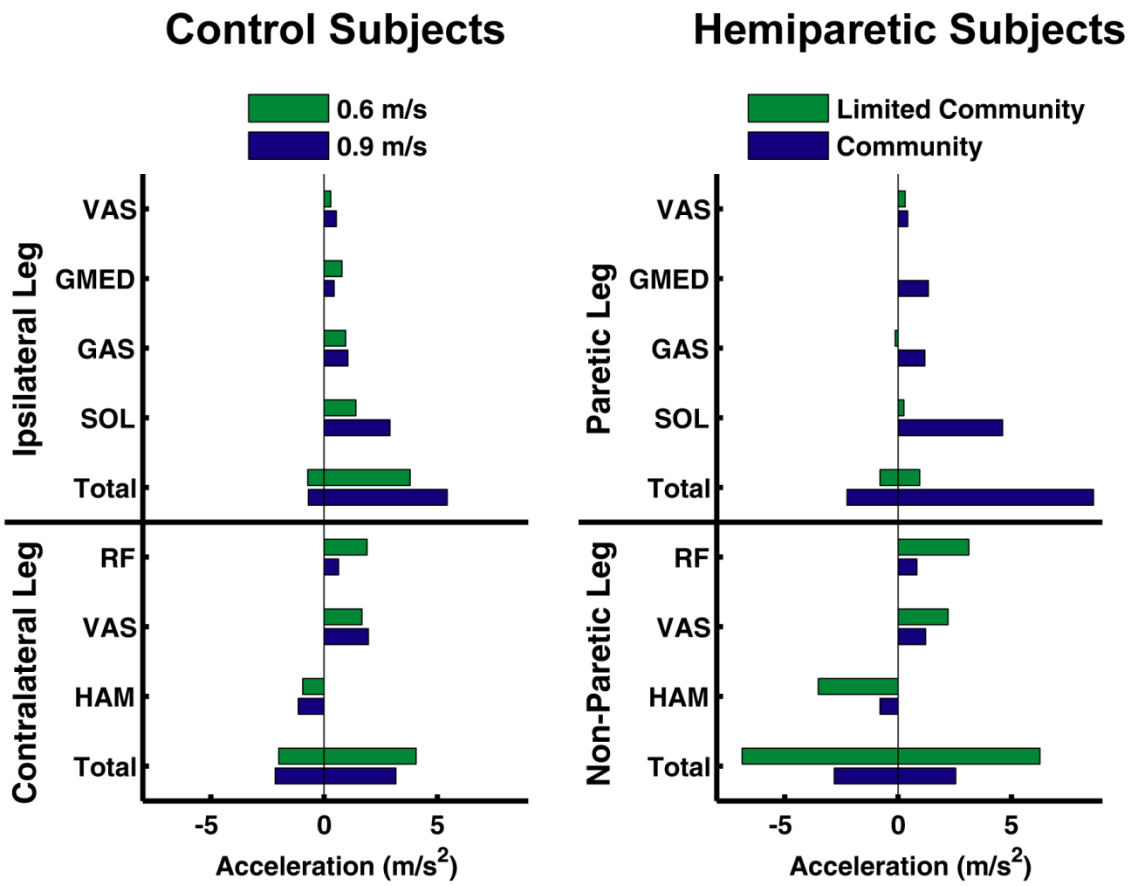

Figure 2.1. Average muscle contributions to forward propulsion (i.e., horizontal pelvis acceleration) by the control subjects during the ipsilateral pre-swing phase and the hemiparetic subjects during the paretic pre-swing phase, where Total is the positive and negative sums from all muscles for the respective leg. Contributions from the ipsilateral leg muscles to forward propulsion increased as walking speed increased from 0.6 to 0.9 m/s in the control subjects. Similarly, contributions from the paretic leg muscles (i.e., SOL, GAS and GMED) to forward propulsion increased with improved functional walking status. The non-paretic leg muscles (i.e., RF and VAS) contributed to forward propulsion in the limited community walkers to compensate for reduced paretic leg muscle contributions.

Swing Initiation

In the control subjects, both the ipsilateral and contralateral leg muscles increased their positive contributions to swing initiation with increased walking speed (Fig. 2.2: Total). In the control subjects, the ipsilateral and contralateral leg muscles' negative contributions to swing initiation increased and decreased, respectively, as walking speed increased from 0.6 to 0.9 m/s (Fig. 2.2: Total).

In the hemiparetic subjects, positive contributions to swing initiation from the paretic and non-paretic leg muscles increased as functional walking status improved (Fig. 2.2: Total). Negative contributions to swing initiation from the paretic and non-paretic leg muscles increased and decreased, respectively (Fig. 2.2: Total).

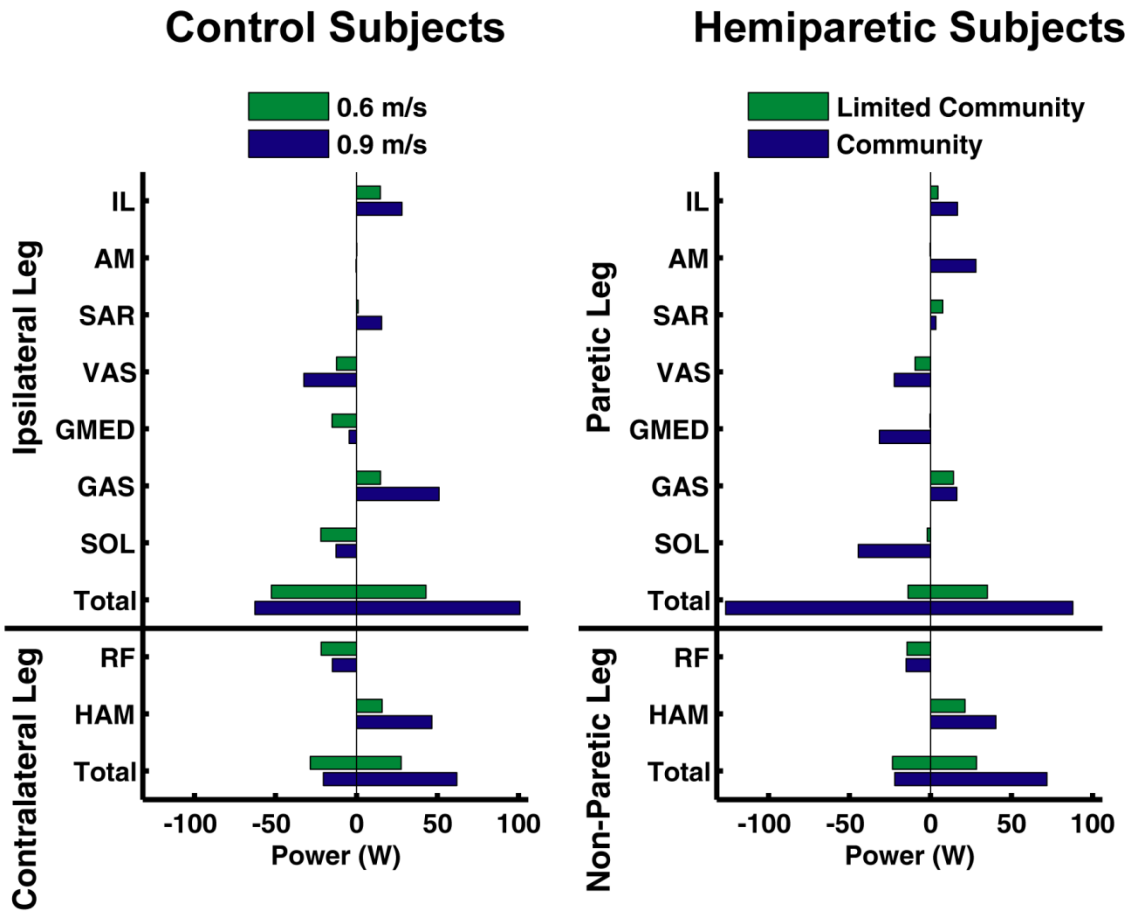

Figure 2.2. Average muscle contributions to swing initiation (i.e., net power transferred to/from the ipsilateral/paretic leg) by the control subjects during the ipsilateral pre-swing phase and the hemiparetic subjects during the paretic pre-swing phase, where Total is the positive and negative sums from all muscles for the respective leg. In the control subjects, both the ipsilateral leg muscles (i.e., GAS, IL and SAR) and contralateral leg muscles (i.e., HAM) increased their contributions to swing initiation with increased walking speed. In a similar manner, both the paretic leg muscles (i.e., GAS and IL) and non-paretic leg muscles (i.e., HAM) increased their contributions to swing initiation with improved functional walking status. In the community walkers, paretic AM and GMED contributed positively and negatively, respectively to swing initiation, while these muscles did not contribute to swing initiation in the limited community walkers.

Power Generation

In the control subjects, ipsilateral and contralateral leg muscles increased power generation as speed increased from 0.6 m/s to 0.9 m/s (Fig. 2.3: Total). Power absorption increased in the ipsilateral leg and did not change in the contralateral leg, with increased walking speed (Fig. 2.3: Total).

Paretic and non-paretic leg muscles generated more power as functional walking status improved (Fig. 2.3: Total). Power absorption was increased and did not change with improved functional walking status in the paretic and non-paretic legs, respectively (Fig. 2.3: Total).

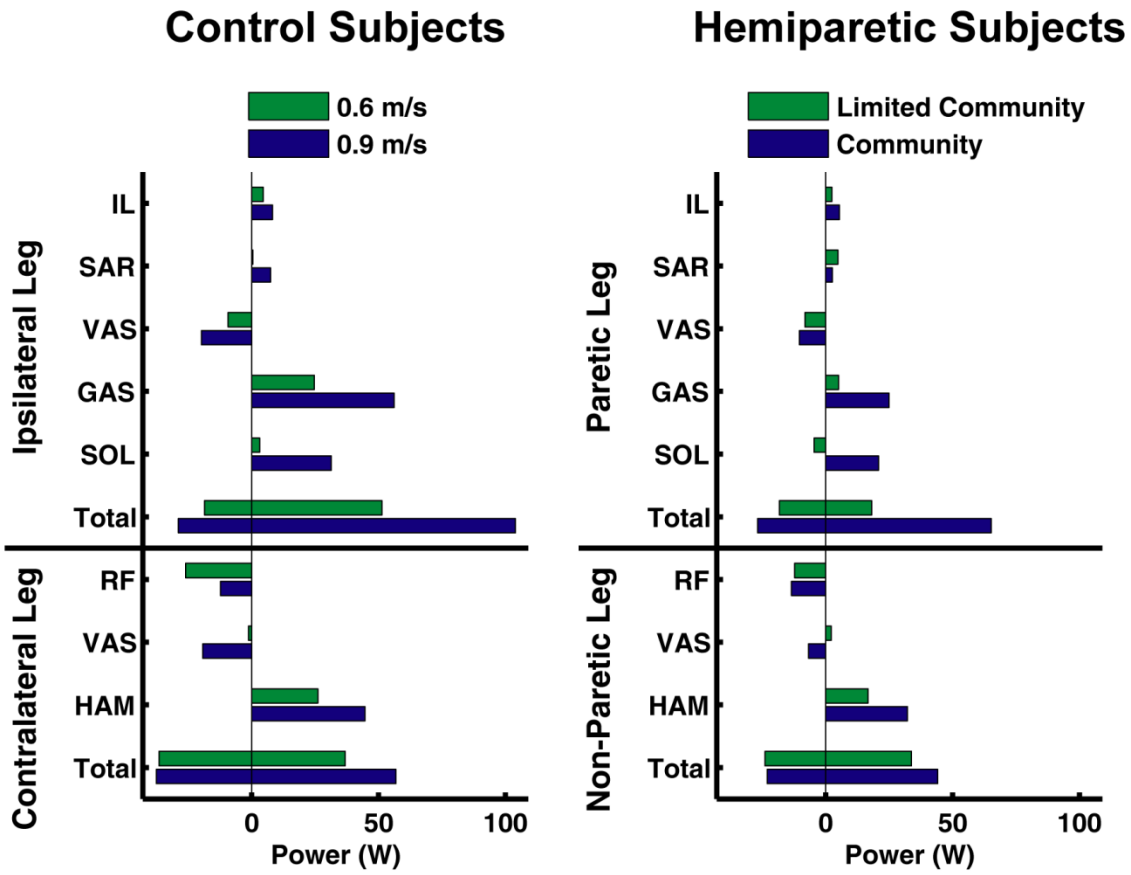

Figure 2.3. Average power generation (i.e., net musculotendon power) by the control subjects during the ipsilateral pre-swing phase and the hemiparetic subjects during the paretic pre-swing phase, where Total is the positive and negative sums from all muscles for the respective leg. Power generation by the ipsilateral leg muscles (i.e., SOL, GAS, IL and SAR) and the contralateral leg muscles (i.e., HAM) increased in the control subjects as speed increased from 0.6 to 0.9 m/s. In the hemiparetic subjects, as functional walking status improved, the paretic leg muscles (i.e., SOL and GAS) and the non-paretic leg muscles (i.e., HAM) generated more power.

Discussion

The purpose of this study was to use 3D muscle-actuated forward dynamics simulations to determine differences in forward propulsion, swing initiation and power generation during the pre-swing phase between hemiparetic subjects and age and speed-

matched controls to identify differences in muscle coordination associated with improved functional walking status. The results showed that decreased paretic leg muscle contributions to the walking subtasks were associated with functional walking status in the hemiparetic subjects.

In both the control and hemiparetic subjects, ipsilateral (paretic) SOL was an important contributor to forward propulsion during pre-swing and was critical to increasing walking speed and corresponded with higher functional walking status (Fig. 2.1). This result is consistent with previous studies showing SOL to be a primary contributor to forward propulsion (e.g., McGowan et al., 2008; Neptune et al., 2001) and a mechanism for attaining higher walking speeds in healthy walking (Liu et al., 2008; Neptune et al., 2008) and in the hemiparetic population (Nadeau et al., 1999; Olney et al., 1991; Parvataneni et al., 2007). The contralateral (non-paretic) VAS also had a large contribution to forward propulsion during the ipsilateral (paretic) leg pre-swing phase in the control (hemiparetic) subjects (Fig. 2.1). As a result, both ipsilateral (paretic) SOL and contralateral (non-paretic) VAS were important determinants of walking speed in our subjects.

In the hemiparetic subjects, a strong relationship was found between the contribution of the paretic leg muscles to forward propulsion and functional walking status. In the community walkers, the paretic leg muscles generated the majority of the forward propulsion as seen with the control subjects (Fig. 2.1). However, the limited community walkers' muscle contributions were altered compared to the community walkers and the control subjects, with the paretic leg muscles (SOL, GAS and GMED) contributing little to forward propulsion and the non-paretic leg muscles (RF and VAS) compensating for the reduced paretic leg output (Fig. 2.1). This result is consistent with Bowden et al (2006) who showed that the non-paretic leg's contribution to the AP GRF

increased as hemiparetic severity increased. In addition, the non-paretic leg muscles (primarily HAM) increased their contributions to pelvis deceleration in the limited community walkers compared to the community walkers, resulting in a net (sum of all paretic and non-paretic leg muscles) deceleration of the pelvis during pre-swing.

Leg swing initiation was provided primarily by ipsilateral GAS, IL and contralateral HAM in the control subjects and increased contribution from these muscles was required to increase walking speed from 0.6 to 0.9 m/s (Fig. 2.2), which is consistent with previous simulations of healthy walking at self-selected speed (e.g., Neptune et al., 2001; Neptune et al., 2004) and increased walking speeds (Neptune et al., 2008). In the hemiparetic subjects, these muscles have a clear impact on functional walking status. The community walkers' muscle contributions to swing initiation were similar to the muscle contributions seen in the control subjects with paretic GAS, IL and contralateral HAM contributing strongly to paretic leg swing initiation. In addition to these muscles, AM and GMED contributed positively and negatively, respectively, to swing initiation. The contributions from AM and GMED were similar in magnitude and resulted in a small net negative contribution (-3.5 W) to swing initiation. Clear deficits existed in the paretic and non-paretic leg muscle contributions to swing initiation in the limited community walkers (Fig. 2.2), which is consistent with previous studies that have shown reduced paretic leg kinetic energy at toe-off, suggesting impaired swing initiation in the paretic leg (e.g., Chen and Patten, 2008). Paretic GAS, IL and non-paretic HAM contributions were reduced in the limited community walkers compared to the community walkers (Fig. 2.2). The negative contributions from the paretic leg muscles (VAS, GMED, SOL) were also greatly reduced (Fig. 2.2) in the limited community walkers, allowing the leg to accelerate into swing.

Power generation by both ipsilateral and contralateral leg muscles during pre-swing in the control subjects generally increased with walking speed (Fig. 2.3) and showed consistent trends to previous studies (e.g., Neptune et al., 2004; Neptune et al., 2008). Power generation was also an important indicator of functional walking status in the hemiparetic subjects. Power generation by muscles in the community walkers closely resembled those of the control subjects. However, in the limited community walkers, the paretic leg muscles, specifically GAS and IL, generated less power, consistent with their reduced contributions to forward propulsion (GAS) and swing initiation (GAS and IL). In addition, paretic SOL absorbed power in the limited community walkers in contrast with the community walkers and control subjects, where it generated power in pre-swing. The power absorption by SOL in the limited community walkers limited its ability to contribute to forward propulsion.

The limitations of forward dynamics simulations and analyses have been previously discussed (e.g., Neptune et al., 2001; Neptune et al., 2004), including necessary modeling assumptions and constraints. Specific to this study, a potential limitation is that model parameters for all the simulations were based on measurements obtained from healthy control subjects. It is likely that these properties are altered post-stroke, as has been shown in a recent study (Gao et al., 2009). However, the optimization was able to compensate for altered model properties by modulating the magnitude of the muscle excitation to produce the necessary muscle force output to replicate the subject's walking mechanics. Also, the results of this study are specific to hemiparetic subjects who walk with similar kinematic and kinetic patterns to the subjects simulated in this study. Because of the heterogeneity of the post-stroke hemiparetic population, the extent to which these results can be generalized to the post-stroke population as a whole is not clear. Future work should focus on developing simulations of a larger number of

hemiparetic subjects to gain further insight into the changes in muscle function in this population.

In summary, the analyses showed that deficits in the walking subtasks of forward propulsion, swing initiation and power generation are related to functional walking status in hemiparetic walking. Increased contributions from the paretic leg muscles (i.e., plantarflexors and hip flexors) and reduced contributions from the non-paretic leg (i.e., knee and hip extensors) to the walking subtasks were critical in achieving higher functional walking status. These results provide rationale for developing rehabilitation strategies that focus on these muscle groups in order to improve the functional walking status of persons with post-stroke hemiparesis.

Chapter 3: Changes in Muscle Contributions to Propulsion in Post-Stroke Hemiparetic Walking Pre- and Post-Locomotor Training

Introduction

A common goal of post-stroke rehabilitation is to improve walking speed in hemiparetic subjects and numerous studies have shown that post-stroke rehabilitation is effective in accomplishing this goal (Ada et al., 2003; Barbeau and Visintin, 2003; Mulroy et al., 2010; Parvataneni et al., 2007; Peurala et al., 2005; Sullivan et al., 2007; Teixeira-Salmela et al., 2001; Visintin et al., 1998). However, improvements in walking speed can be obtained through several mechanisms including increased propulsion in either the paretic and non-paretic legs. Hemiparetic subjects have altered anterior-posterior ground reaction forces (AP GRFs) in comparison to healthy subjects, with the paretic leg contribution to the AP GRF positively correlated with hemiparetic walking speed and an important indicator of hemiparetic severity (Bowden et al., 2006). However, it is unclear how individual muscles contribute to the AP GRFs in hemiparetic walking and how the contributions change during rehabilitation to improve walking speed.

Previous studies of joint kinetics have shown that hemiparetic subjects are able to increase paretic leg ankle plantarflexor power to improve walking speed post-rehabilitation (Mulroy et al., 2010; Parvataneni et al., 2007; Teixeira-Salmela et al., 2001). Modeling and simulation studies of healthy walking have also shown that the contributions of the ankle plantarflexors (soleus, SOL and gastrocnemius, GAS), to propulsion increase with walking speed (Liu et al., 2008; Neptune et al., 2008). Thus, it is expected that hemiparetic subjects who improve walking speed by increasing paretic leg propulsion may have increased contributions from the paretic leg ankle plantarflexors (SOL and GAS).

Hemiparetic subjects with moderate and high severity have been shown to rely more on their non-paretic leg to generate propulsion (Bowden et al., 2006). Previous simulation studies of healthy walking have shown that the hamstrings (HAM) contribute positively to propulsion (i.e., anterior-posterior acceleration of the body center-of-mass (COM)) from early to mid-stance (Liu et al., 2008; Neptune et al., 2004) and that the gluteus maximus (GMAX) and vastii (VAS) muscles contribute to trunk forward propulsion during foot-flat (Neptune et al., 2004). Experimental studies have also shown that hemiparetic subjects increase non-paretic leg hip extensor power in early stance following rehabilitation (Parvataneni et al., 2007; Teixeira-Salmela et al., 2001). Therefore, it is expected that some hemiparetic subjects who improve walking speed by increasing non-paretic leg propulsion may have increased contributions from the non-paretic leg hip and knee extensors (HAM, GMAX and VAS) during late paretic leg stance (i.e., early non-paretic leg stance).

The hemiparetic population is heterogeneous and has been shown to use different strategies to generate propulsion, with some subjects generating high paretic leg propulsion, while others generate low paretic leg propulsion (Bowden et al., 2006). Subjects who generate high paretic leg propulsion typically have mild hemiparesis and walk at faster speeds than other hemiparetic subjects (Bowden et al., 2006), consistent with limited paretic leg ankle plantarflexor impairment. Therefore, subjects who generate high paretic leg propulsion pre-training may be more likely to improve walking speed during rehabilitation by increasing paretic leg propulsion. However, subjects who generate lower paretic leg propulsion typically walk at slower speeds (Bowden et al., 2006) and have increased non-paretic leg muscle contributions to forward propulsion (Hall et al., 2010; Peterson et al., 2010). Therefore, subjects who generate low paretic leg

propulsion pre-training may be more likely to increase non-paretic leg propulsion to improve walking speed during rehabilitation.

The purpose of this study was to investigate muscle contributions to propulsion (as measured by AP COM acceleration) from mid to late paretic leg stance in hemiparetic subjects pre- and post-locomotor training to understand the changes in muscle coordination that lead to improved walking speed during rehabilitation. Forward dynamics simulations have successfully identified individual muscle contributions to increased walking speed in healthy walking (Liu et al., 2008; Neptune et al., 2008) and to pelvis forward acceleration (Hall et al., 2010; Peterson et al., 2010) and body support (Higginson et al., 2006) in hemiparetic walking. However, the studies that have investigated post-stroke hemiparetic walking developed simulations that were limited in duration and only included a few individual subjects (Higginson et al., 2006; Peterson et al., 2010) or group average data (Hall et al., 2010) in the analysis. This study will develop a large number of subject-specific forward dynamics simulations of hemiparetic walking over the complete gait cycle. In addition, no study has investigated individual muscle contributions to body propulsion pre- and post-locomotor training and determined how the contributions change during rehabilitation to gain insight into the mechanisms of response to locomotor rehabilitation training. By identifying the changes in muscle coordination necessary to improve walking speed in a large number of subject-specific simulations, this study will provide insight into the variability across hemiparetic subjects and the strategies that emerge to increase walking speed during rehabilitation.

Methods

Subjects

Ten hemiparetic subjects (6 left hemiparesis; 8 men; age: mean = 59.8 years (SD = 12.1 years); time since stroke: mean = 21.6 months (SD = 16.3 months)) who completed a 12-week locomotor training intervention at the VA Brain Rehabilitation Research Center at the Malcom Randall VA Medical Center (Gainesville, FL) were included in this study. Subject characteristics for the hemiparetic subjects are provided in Table B4 in Appendix B. Inclusion criteria for the hemiparetic subjects were: 1) at least 18 years of age, 2) stroke within past 6 months - 5 years, 3) residual paresis in the lower extremity (Fugl-Meyer LE motor score < 34), 4) ability to sit unsupported for 30 seconds, 5) ability to walk at least 10 feet with maximum 1 person assist, 6) self-selected 10-meter gait speed less than 0.8 m/s, 7) ability to follow a three step command. All subjects passed an exercise tolerance test (Yates et al., 2004) to verify their cardiovascular fitness prior to participation. All subjects provided written informed consent approved by the Institutional Review Boards of the University of Florida and the University of Texas at Austin.

Locomotor Training Intervention

Each subject participated in a 12-week locomotor training intervention consisting of training sessions three times a week. During each session, subjects participated in 20 minutes of walking using a body-weight supported treadmill training (BWSTT) modality (Hesse et al., 1995; Plummer et al., 2007; Visintin et al., 1998) followed by 20 minutes of immediate translation of skills acquired during treadmill walking to overground walking. During BWSTT, subjects wore a safety harness to protect against a loss of balance.

BWSTT began with 40% BWS and progressed as tolerated to no BWS. BWSTT took place at 2.0 – 3.0 mph with manual assistance provided by physical therapists at the hip and/or lower legs to approximate desired trunk, pelvis and lower limb kinematics and the spatio-temporal pattern of walking (Plummer et al., 2007).

Experimental Data Collection and Analysis

Each subject walked on an ADAL split-belt instrumented treadmill (Tecmachine, Andrézieux Bouthéon, France) while data were collected for 30 seconds (Appendix C). Subjects walked at both self-selected and fastest-comfortable speeds both pre- and post-training. Experimental data collected at the fastest-comfortable speed were used to develop the simulations. All trials were performed without the use of an assistive device or ankle-foot orthosis. All subjects wore a safety harness mounted to the laboratory ceiling to protect against a loss of balance (no body weight was offloaded by the harness). A physical therapist was present for all data collection sessions. All data were collected using Vicon Workstation v4.5 software (Vicon Motion Systems, Oxford, UK) and processed using Visual3D (C-motion, Inc., Germantown, MD). 3D GRF data were measured at 2000 Hz from piezoelectric sensors (Kistler, Winterthur, Switzerland) on each half of the treadmill and low-pass filtered with a fourth-order Butterworth filter with a cutoff frequency of 20 Hz. Reflective markers were placed on the head (top, left and right temple and back), trunk (C7, T10, clavicle, sternum and right scapula) and arms (left and right shoulder, elbow and wrist). Clusters of reflective markers were attached to the pelvis and left and right thigh, shank and foot segments. Marker trajectories were recorded at 100 Hz with a 12-camera motion capture system (Vicon Motion Systems, Oxford, UK) and low-pass filtered with a fourth-order Butterworth filter with a cutoff

frequency of 6 Hz. Surface electromyographic (EMG) data were recorded bilaterally at 2000 Hz from the tibialis anterior, medial gastrocnemius, soleus, rectus femoris, biceps femoris long head, vastus medialis, semimembranosus and gluteus medius using a 16-channel EMG system (Konigsburg Instruments, Pasadena, CA). The raw EMG data were high-pass filtered at 40 Hz, demeaned, rectified and low-pass filtered with a fourth-order Butterworth filter with a cutoff frequency of 4 Hz.

For each trial simulated, an inverse kinematics analysis was performed in Visual3D for input into OpenSim (Delp et al., 2007). Experimental kinematics and GRFs were normalized to the paretic leg gait cycle and averaged across gait cycles. A representative gait cycle with the smallest difference in kinematics and GRFs from the average data was chosen for the tracking data in the optimization. The EMG data were used to constrain the timing (onset and offset) of the muscle excitation patterns in the optimization to ensure muscles were producing force at the appropriate point in the gait cycle. For those muscles where EMG data were not available, data from the literature (den Otter et al., 2004; den Otter et al., 2007; Perry et al., 1995; Sutherland, 1984) were used.

Musculoskeletal Model

A bipedal 3D musculoskeletal model with 19 degrees-of-freedom was used to generate forward dynamics walking simulations of the hemiparetic subjects pre- and post-training. The generic model geometry and anthropometry were based on Delp et al. (1990) and Anderson and Pandy (1999; 2001). Scale factors were calculated for each subject in Visual3D by comparing the segment lengths measured during a static calibration trial and the segment geometry in the generic musculoskeletal model. The

scale factors were then used to generate subject-specific models scaled for each subject. The model included 12 rigid segments representing the trunk, pelvis and two legs (thigh, shank, talus, calcaneus and toes). The pelvis had 6 degrees-of-freedom (3 translations and 3 rotations) and the trunk and hip joints were modeled as spherical joints. The knee joints were modeled as planar joints with the tibiofemoral translations defined as a function of knee flexion angle (Yamaguchi and Zajac, 1989). The ankle joints were modeled as single degree-of-freedom revolute joints.

The musculoskeletal model was actuated by 92 individual Hill-type musculotendon actuators with 6 trunk muscles and 43 muscles per leg (Table 3.1). The muscle contraction dynamics were governed by Hill-type muscle properties (Zajac, 1989). The activation dynamics were modeled by a first-order differential equation (Raasch et al., 1997), with nominal activation and deactivation time constants of 10 and 40 ms, respectively.

Table 3.1. The 92 musculotendon actuators in the musculoskeletal model were combined into 21 after analysis according to anatomical classification.

Muscle Name	Analysis Group
Iliacus	IL
Psoas	IL
Adductor Longus	AL
Adductor Brevis	AL
Pectineus	AL
Quadratus Femoris	QF
Superior Adductor Magnus	AM
Middle Adductor Magnus	AM
Inferior Adductor Magnus	AM
Sartorius	SAR
Rectus Femoris	RF
Vastus Medialis	VAS
Vastus Lateralis	VAS
Vastus Intermedius	VAS
Anterior Gluteus Medius	GMED
Middle Gluteus Medius	GMED
Posterior Gluteus Medius	GMED
Piriformis	PIRI
Gemellus	GEM
Anterior Gluteus Minimus	GMIN
Middle Gluteus Minimus	GMIN
Posterior Gluteus Minimus	GMIN
Tensor Fascia Lata	TFL
Anterior Gluteus Maximus	GMAX
Middle Gluteus Maximus	GMAX
Posterior Gluteus Maximus	GMAX
Semitendinosus	HAM
Semimembranosus	HAM
Gracilis	HAM
Biceps Femoris Long Head	HAM
Biceps Femoris Short Head	BFSH
Medial Gastrocnemius	GAS
Lateral Gastrocnemius	GAS
Soleus	SOL
Tibialis Posterior	SOL
Peroneus Brevis	SOL
Peroneus Longus	SOL
Flexor Digitorum Longus	SOL
Flexor Hallucis Longus	SOL
Tibialis Anterior	TA
Extensor Digitorum Longus	TA
Peroneus Tertius	TA
Extensor Hallucis Longus	TA
Erector Spinae	ERSP
External Oblique	EXOB
Internal Oblique	INOB

Generation of Forward Dynamics Simulations

Forward dynamics simulations of each subject walking pre- and post-training were developed using OpenSim (Delp et al., 2007) and simulated consecutive paretic and non-paretic stance phases. The following procedure was executed for each trial simulated. Three external forces and three external moments (i.e., residuals) were applied at the pelvis to minimize the dynamic inconsistency between the experimentally measured kinematics and GRFs. In addition, reserve torque actuators were applied at each joint to represent the forces applied by the ligaments, passive tissues and joint structures. To reduce the magnitudes of the residuals, a residual reduction algorithm (RRA) was applied to adjust the scaled model's mass, the torso center-of-mass location and the tracking kinematics. A computed muscle control (CMC) algorithm (Thelen et al., 2003; Thelen and Anderson, 2006) was used to compute the actuator (muscles, reserve torques and residual forces and moments) controls that reproduce the desired experimental kinematics.

Analysis of Muscle Function

For each trial simulated, a perturbation analysis (Liu et al., 2006) was performed to determine the individual muscle contributions to the AP accelerations of the body COM. At each time step in the simulation, an individual muscle's contribution to the COM acceleration was determined by perturbing the musculotendon force by 1 N, integrating forward by 20 ms, and calculating the resulting change in COM position. By assuming that the acceleration was constant over the integration time step (Δt), the muscle-induced COM acceleration was calculated as:

$$\ddot{x}(t) \approx 2 \cdot \frac{x(F_m+\Delta F_m, t+\Delta t) - x(F_m, t+\Delta t)}{\Delta t^2 \Delta F_m} F_m \qquad (3.1)$$

where F_m is the force generated by muscle m and ΔF_m is the 1 N perturbation to F_m. Each muscle's contribution to propulsion was determined as the average contribution to the AP COM acceleration during the late single-limb stance region (i.e., second half of paretic leg single-limb stance) and pre-swing region (i.e., double support region preceding paretic leg toe-off). Contributions from individual muscles were grouped after analysis according to anatomical function (Table 3.1). Subjects were divided into groups based on their pre-training propulsion symmetry, defined as the percent of paretic propulsion (PP = positive paretic AP impulse/(positive paretic + positive non-paretic AP impulse)). Muscle group contributions from subjects in the low ($n = 7$, $PP < 0.45$) and high ($n = 3$, $PP > 0.55$) PP groups were averaged in both the late single-limb stance and pre-swing regions. The average data from each group were compared between pre-training and post-training sessions to determine the changes in muscle coordination during rehabilitation and identify the strategies that each group used to improve walking speed.

Results

The average fastest-comfortable walking speed for the hemiparetic subjects improved from 0.49 m/s (SD = 0.22 m/s) to 0.75 m/s (SD = 0.24 m/s) during rehabilitation. The kinematic data from the pre- and post-training simulations agreed well with the experimental data, with an average absolute error over the simulation duration of 0.53 degrees and 0.56 degrees, respectively (Table 3.2). As in previous studies (Neptune et al., 2001; Neptune et al., 2004), the timing of the optimized excitation patterns generally agreed with the experimentally collected EMG data. At both pre- and post-training, the simulated AP COM accelerations were consistent with the experimental

AP COM accelerations (Figs. 3.1 and 3.2, see Net Simulation and Net Experimental). During the late single-limb stance region, muscles and gravity provided 82.0% and 81.2% of the simulated AP COM acceleration for the pre- and post-training simulations, respectively. The reserve and residual actuators provided 18.0% and 18.8% of the simulated AP COM acceleration during the late paretic leg single-limb stance region for the pre- and post-training simulations, respectively. During the paretic leg pre-swing region, the majority (92.9% and 93.2% for the pre- and post-training simulations, respectively) of the simulated AP COM acceleration was provided by the muscles and gravity. Reserve and residual actuators provided an average of 7.1% and 6.8% of the AP COM accelerations in the paretic leg pre-swing region of the pre- and post-training simulations, respectively.

Table 3.2. The average difference between the experimental and simulated kinematic angles (Simulated Error) compared to the average standard deviation of the experimental data (Experimental Error) for all subjects. The errors were calculated over the entire duration of the simulation.

		Pre-Training		Post-Training	
Kinematic Angles (degrees)		**Simulated Error**	**Experimental Error**	**Simulated Error**	**Experimental Error**
Pelvis	**Tilt**	0.41	1.47	0.15	1.33
	List	0.31	1.14	0.11	1.14
	Rotation	0.28	2.56	0.24	2.21
Paretic Leg	**Hip Flexion**	1.12	2.32	1.36	2.86
	Hip Adduction	0.31	1.14	0.40	1.33
	Hip Rotation	0.16	2.12	0.21	2.24
	Knee Angle	0.63	3.25	0.88	3.70
	Ankle Angle	0.96	1.88	0.57	1.81
Non-Paretic Leg	**Hip Flexion**	0.98	2.72	1.29	3.15
	Hip Adduction	0.31	1.29	0.36	1.39
	Hip Rotation	0.21	2.04	0.25	2.09
	Knee Angle	0.55	3.66	0.48	3.83
	Ankle Angle	0.44	2.00	0.42	2.16
Lumbar	**Extension**	1.12	0.69	1.37	0.69
	Bending	0.36	1.38	0.40	1.37
	Rotation	0.29	1.03	0.42	1.21
Average		0.53	1.92	0.56	2.03
Standard Deviation		0.33	0.84	0.43	0.94

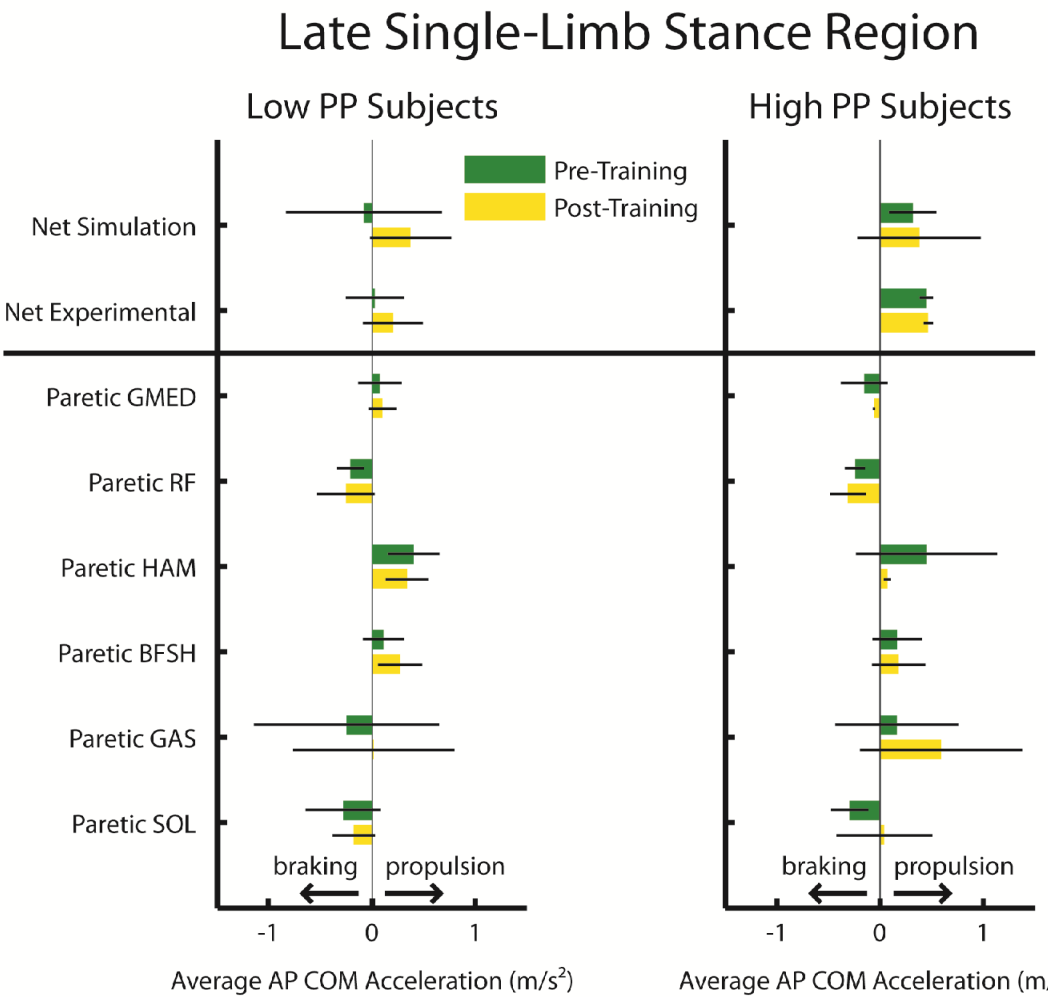

Figure 3.1. Average muscle contributions to propulsion (i.e., positive anterior-posterior (AP) body center-of-mass (COM) acceleration) and braking (i.e., negative AP body COM acceleration) during the late single-limb stance region (i.e., second half of paretic leg single-limb stance) for the subjects with low paretic propulsion (PP) and high PP pre-training. Net Simulation and Net Experimental represent the average body COM acceleration from the simulation and experimental data, respectively.

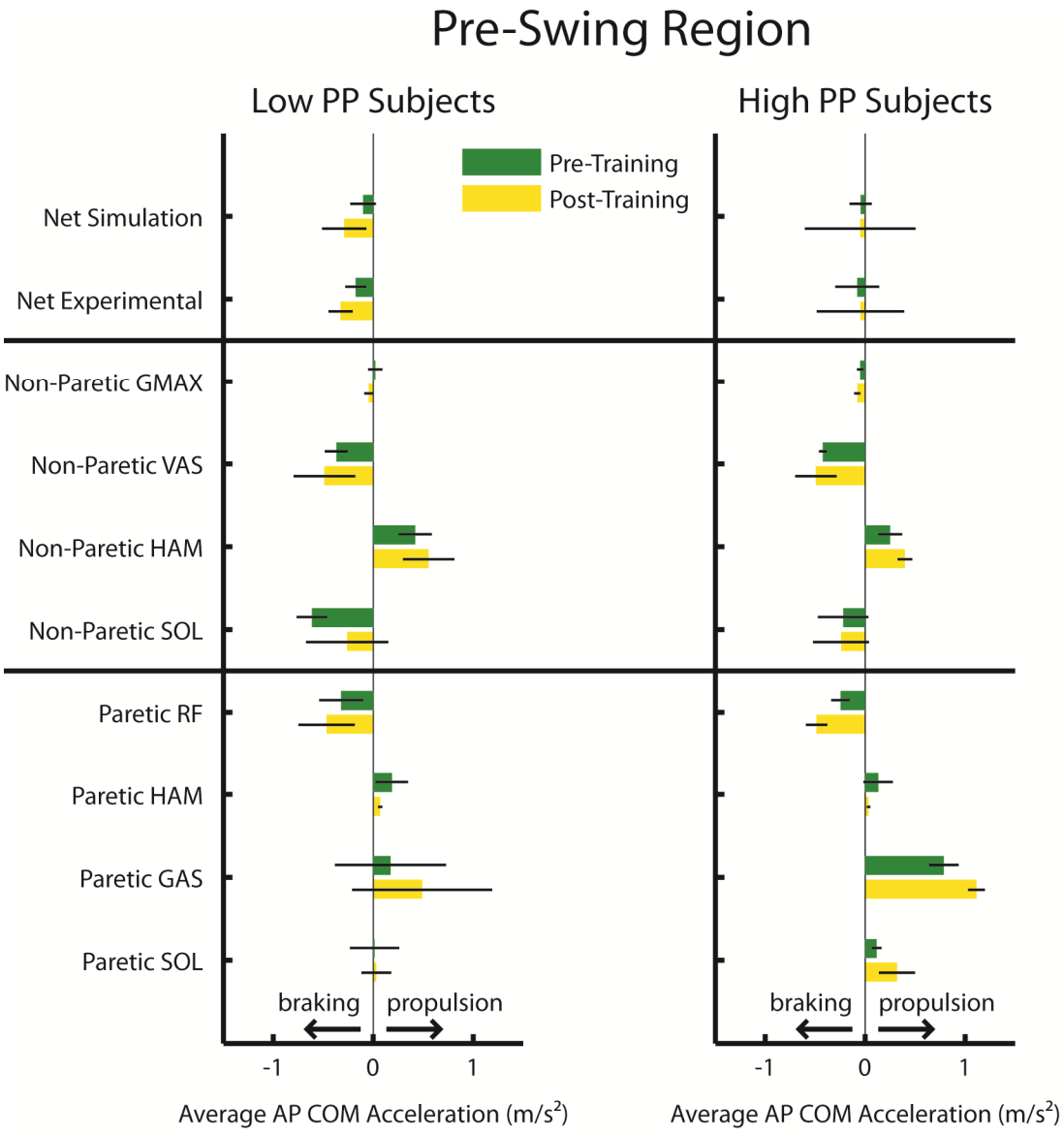

Figure 3.2. Average muscle contributions to propulsion (i.e., anterior-posterior (AP) body center-of-mass (COM) acceleration) and braking (i.e., negative AP body COM acceleration) during the pre-swing region (i.e., double support region preceding paretic leg toe-off) for the subjects with low paretic propulsion (PP) and high PP pre-training. Net Simulation and Net Experimental represent the average body COM acceleration from the simulation and experimental data, respectively.

Muscle Contributions to Propulsion from the Low PP Subjects

For the low PP subjects, paretic leg HAM, BFsh and GMED were the primary contributors to propulsion during late paretic leg single-limb stance at the pre-training session (Fig. 3.1). Paretic leg BFsh increased its contribution to propulsion during late paretic leg single-limb stance from pre- to post-training while contributions from paretic leg HAM and GMED did not change during training (Fig. 3.1).

The primary contributors to braking (i.e., AP COM deceleration) during the late paretic leg single-limb stance region at the pre-training session were paretic leg SOL, GAS and RF (Fig. 3.1). At the post-training session, contributions to braking during late paretic leg single-limb stance from paretic leg SOL and GAS were reduced and contributions from paretic leg RF did not change relative to the pre-training session for the low PP subjects (Fig. 3.1).

At the pre-training session, non-paretic leg HAM and paretic leg HAM and GAS were the primary contributors to propulsion during paretic leg pre-swing in the low PP subjects (Fig. 3.2). Contributions from paretic leg GAS and non-paretic leg HAM increased from pre- to post-training, while contributions from paretic leg HAM decreased in the paretic leg pre-swing region (Fig. 3.2). Paretic leg SOL and non-paretic GMAX also contributed positively to paretic leg pre-swing propulsion at the pre-training session, although the contributions were small and did not change during training (Fig. 3.2).

Non-paretic leg SOL and VAS and paretic leg RF were the primary contributors to braking during the paretic leg pre-swing region at the pre-training session (Fig. 3.2). At the post-training session, contributions during the paretic leg pre-swing region from non-paretic leg VAS and paretic leg RF increased relative to the pre-training session (Fig. 3.2). During the paretic leg pre-swing region, non-paretic leg SOL decreased its contribution to braking from pre- to post-training (Fig. 3.2).

Muscle Contributions to Propulsion from the High PP Subjects

Paretic leg HAM, GAS and BFsh were the primary contributors to propulsion during the late paretic leg single-limb stance region for the high PP subjects at the pre-training session (Fig. 3.1). At the post-training session, contributions during late paretic leg single-limb stance from paretic leg HAM decreased and contributions from paretic leg GAS increased relative to the pre-training session (Fig. 3.1). For the high PP subjects, paretic leg BFsh did not change its contribution to propulsion during late paretic leg single-limb stance from pre- to post-training (Fig. 3.1).

During the late paretic leg single-limb stance region, paretic leg SOL, RF and GMED were the primary contributors to braking for the high PP subjects at the pre-training session (Fig. 3.1). The contributions from paretic leg GMED decreased and the contributions from paretic leg RF did not change during training (Fig. 3.1). At the post-training session, the paretic leg SOL contribution for the high PP subjects became positive, contributing to propulsion (Fig. 3.1).

For the high PP subjects, the primary contributions to propulsion during the paretic leg pre-swing region were provided by paretic leg GAS, HAM and SOL and non-paretic leg HAM pre-training (Fig. 3.2). Relative to the pre-training session, contributions from paretic leg GAS and SOL and non-paretic leg HAM increased at the post-training session, while the contribution from paretic leg HAM decreased during training (Fig. 3.2).

The primary contributors to braking during the paretic leg pre-swing region at the pre-training session were non-paretic leg VAS and SOL and paretic leg RF (Fig. 3.2). At the post-training session, contributions from non-paretic leg VAS and SOL did not change and contributions from paretic leg RF increased relative to the pre-training session (Fig. 3.2). For the high PP subjects, non-paretic leg GMAX also contributed to

braking, but the contribution was small and did not change from pre- to post-training (Fig. 3.2).

Discussion

The purpose of this study was to use a large number of subject-specific 3D muscle-actuated forward dynamics simulations of hemiparetic subjects pre- and post-locomotor training to investigate muscle contributions to propulsion (i.e., AP COM acceleration) from mid to late paretic leg stance to identify the changes in muscle coordination that lead to improved walking speed during rehabilitation. The simulation analyses identified different strategies for increasing walking speed post-rehabilitation in subjects with different levels of pre-training propulsion symmetry.

We expected that hemiparetic subjects who improve walking speed during rehabilitation may have increased contributions to propulsion from the paretic leg ankle plantarflexors (SOL and GAS). During late paretic leg single-limb stance, paretic leg SOL and GAS contributions to propulsion differed, suggesting that the low and high PP subjects generate propulsion differently during this region of the gait cycle. For the low PP subjects, SOL and GAS contributed to braking during late paretic leg single-limb stance and the contributions to braking were reduced from pre- to post-training (Fig. 3.1). The low PP subjects used the reduced braking contributions from the paretic leg ankle plantarflexors to improve speed during late paretic leg single-limb stance, but were unable to generate propulsion from these muscles at post-training, suggesting that the paretic leg ankle plantarflexors are likely impaired in the low PP subjects. For the high PP subjects, paretic leg GAS contributed to propulsion during late paretic leg single-limb stance and the contribution increased with increased walking speed (Fig. 3.1), consistent

with previous studies of healthy walking (Liu et al., 2008; Neptune et al., 2008). Similar to the low PP subjects, paretic leg SOL for the high PP subjects contributed to braking during the late paretic leg single-limb stance region at the pre-training session (Fig. 3.1). However, for the high PP subjects, the paretic leg SOL contribution became positive at the post-training session (Fig. 3.1), contributing to propulsion, which is more consistent with healthy walkers (Liu et al., 2008; Neptune et al., 2008). The high PP subjects relied primarily on the increased paretic leg ankle plantarflexors during late paretic leg single-limb stance to improve propulsion, suggesting that the high PP subjects are able to use this strategy to increase walking speed during rehabilitation.

Both the low and high PP subjects increased contributions to propulsion during the paretic leg pre-swing region from the paretic leg ankle plantarflexors from pre- to post-training (Fig. 3.2), consistent with previous experimental studies that have shown hemiparetic subjects are able to increase paretic leg ankle plantarflexor power to improve walking speed post-rehabilitation (Mulroy et al., 2010; Parvataneni et al., 2007; Teixeira-Salmela et al., 2001). For the high PP subjects, both paretic leg SOL and GAS increased contributions to propulsion during paretic leg pre-swing (Fig. 3.2), consistent with previous simulations studies that showed increased SOL and GAS contributions were critical to achieving higher walking speeds in healthy (Liu et al., 2008; Neptune et al., 2008) and hemiparetic (Hall et al., 2010) walking. However, for the low PP subjects, the pre-swing contributions from paretic leg SOL to propulsion were small both pre- and post-training and did not change during rehabilitation (Fig. 3.2), suggesting that the low PP subjects may have impaired paretic leg SOL force production during paretic leg pre-swing compared to the high PP subjects.

Paretic leg HAM also contributed positively to propulsion for both the low and high PP subjects during the paretic leg late single-limb stance and pre-swing regions,

with contributions decreasing from pre- to post-training in late single-limb stance for the high PP subjects and in pre-swing for both the low and high PP subjects (Figs. 3.1 and 3.2). While the hamstrings are not typically active in late stance in healthy walking, the hemiparetic subjects in this study showed prolonged paretic leg hamstring activity pre-training, consistent with previous analyses of muscle EMG (den Otter et al., 2007). HAM has been shown to contribute positively to propulsion in healthy walking in early stance (Neptune et al., 2004) and the prolonged paretic leg HAM contributions in both the low and high PP subjects may be a compensatory mechanism for increasing paretic leg propulsion pre-training. The decreased contributions at the post-training session for the low PP subjects during paretic leg pre-swing and for the high PP subjects during both regions suggest that this compensatory mechanism was reduced as the ankle plantarflexors increased their contributions to propulsion.

The paretic leg HAM contributions to propulsion did not change during rehabilitation in the low PP subjects in late paretic leg single-limb stance (Fig. 3.1), suggesting that paretic leg HAM may continue to compensate for impaired ankle plantarflexor contributions to propulsion during this region of the gait cycle post-training. Paretic leg BFsh also contributed to propulsion in late paretic leg single-limb stance in both the low and high PP subjects (Fig. 3.1). As BFsh has been shown to act co-functionally with HAM in healthy walking (Neptune et al., 2004), the hemiparetic subjects may be using paretic leg BFsh similarly to contribute to propulsion during late paretic leg single-limb stance.

We also expected that non-paretic leg hip and knee extensors would increase contributions to propulsion during late paretic leg stance (i.e., early non-paretic leg stance) with improved walking speed post-rehabilitation. Non-paretic leg HAM was a primary contributor to propulsion during paretic leg pre-swing for both the low and high

PP subjects with the contribution increasing from pre- to post-training (Fig. 3.2). This result is consistent with previous experimental studies that have shown hemiparetic subjects increase non-paretic leg hip extensor power in early non-paretic leg stance following rehabilitation (Parvataneni et al., 2007; Teixeira-Salmela et al., 2001). For the low PP subjects, non-paretic leg HAM was the top contributor to propulsion during paretic leg pre-swing at both pre- and post-training session (Fig. 3.2). This suggests that non-paretic HAM may be a primary compensatory mechanism for improving walking speed in hemiparetic subjects with low PP pre-training. During the paretic leg pre-swing region, subjects with high PP pre-training also showed increased contributions from non-paretic leg HAM to propulsion during rehabilitation, but relied primarily on the paretic leg ankle plantarflexors to improve walking speed (Fig. 3.2).

For both the low and high PP subjects, non-paretic leg VAS and SOL were the primary contributors to braking during paretic leg pre-swing (Fig. 3.2). Paretic leg RF also contributed to braking in both the paretic leg late single-limb stance and pre-swing regions for the low and high PP subjects (Figs. 3.1 and 3.2). Consistent with previous studies of healthy walking (Liu et al., 2008; Neptune et al., 2008), non-paretic VAS contributed to braking in paretic leg pre-swing (i.e., early non-paretic leg stance). In the low PP subjects, the non-paretic leg VAS contribution in paretic leg pre-swing increased from pre- to post-training. Previous studies of the paretic leg pre-swing region of hemiparetic walking have shown the non-paretic VAS accelerates the pelvis forward while strongly decelerating the leg with the net effect of decelerating the COM (Hall et al., 2010; Peterson et al., 2010). The low PP subjects may be using the increased non-paretic leg VAS contributions to accelerate the pelvis forward during paretic leg pre-swing and improve walking speed during rehabilitation. Non-paretic leg SOL also contributed strongly to braking during the paretic leg pre-swing region, with the

contribution in the low PP subjects decreasing from pre- to post-training. SOL has been shown previously to contribute to braking in healthy walking by decelerating both the leg and trunk segments during early stance (Neptune et al., 2001). The reduced contributions to braking during paretic leg pre-swing from non-paretic SOL in the low PP subjects may be a mechanism for improving walking speed post-rehabilitation. In both paretic leg late single-limb stance and pre-swing regions, paretic leg RF also contributed to braking in both the low and high PP subjects, consistent with previous results showing RF has a negative contribution to braking as it acts to decelerate the leg more than it accelerates the trunk in late stance in healthy walking (Neptune et al., 2004). In addition, RF has been shown to increase contributions to trunk acceleration with walking speed in healthy subjects (Neptune et al., 2008). For both the low and high PP subjects, paretic leg RF increased its contribution to braking during paretic leg pre-swing with increased walking speed, likely to increase forward acceleration of the trunk

A potential limitation of this study is that model parameters for the hemiparetic subjects were based on measurements from healthy control subjects. The model geometry and anthropometry were scaled for each hemiparetic subject, but the model parameters were not altered to account for differences between hemiparetic and control subjects. However, the optimization algorithm can compensate for altered model parameters by modulating the magnitude of the muscle excitation to produce the necessary muscle force output to replicate the subject's walking mechanics. Therefore, the muscle forces used to determine muscle function in the hemiparetic subjects are relatively insensitive to the model parameters. In addition, the results of this study are specific to hemiparetic subjects who walk with similar kinematic and kinetic patterns to the subjects simulated in this study. By developing a large number of simulations of hemiparetic walking pre- and post-training to identify the changes in muscle

contributions to propulsion, the results of this study have provided the first step towards understanding the various strategies used by hemiparetic subjects to improve walking speed during rehabilitation. Future work should focus on investigating the impact of rehabilitation on other walking subtasks (e.g., leg swing initiation and body support) that are critical for improving mobility in the post-stroke hemiparetic population.

In summary, the analyses showed that hemiparetic subjects use different strategies to increase walking speed post-rehabilitation. The low PP subjects were unable to generate propulsion from the paretic leg ankle plantarflexors during late paretic leg single limb stance at both pre- and post-training sessions and relied on reduced paretic leg ankle plantarflexor contributions to braking and other paretic leg muscles (HAM and BFsh) to improve propulsion during this region of the gait cycle. Subjects with low PP pre-training showed increased contributions from paretic leg muscles (GAS and RF) and non-paretic leg muscles (HAM) to propulsion during paretic leg pre-swing to improve walking speed post-rehabilitation. The low PP subjects relied primarily on non-paretic leg HAM and paretic leg GAS to generate propulsion both pre- and post-training and were unable to increase pre-swing contributions from paretic leg SOL during rehabilitation, suggesting that these subjects may increase walking speed by increasing both paretic and non-paretic leg propulsion. In both the paretic leg late single-limb stance and pre-swing regions, subjects with high PP pre-training showed increased contributions to propulsion from both paretic leg ankle plantarflexors (SOL and GAS) to improve walking speed during rehabilitation, suggesting that these subjects are more likely to improve walking speed with increased paretic leg propulsion. By investigating the changes in muscle contributions to propulsion used by hemiparetic subjects to increase walking speed post-rehabilitation, this study has revealed two primary strategies that hemiparetic subjects use to improve mobility post-rehabilitation. In addition, by

identifying strategies for subjects with different levels of pre-training propulsion symmetry, the results of this study provide rationale for developing post-stroke rehabilitation that is tailored to an individual subjects' specific needs to improve outcomes.

Chapter 4: Post-Training Biomechanical Predictors of Walking Performance 6-Months Following Post-Stroke Rehabilitation

Introduction

Persons with post-stroke hemiparesis usually have reduced walking speed compared to control subjects and asymmetry between their paretic and non-paretic legs (e.g., Olney and Richards, 1996). Improving walking ability is a priority for post-stroke hemiparetic patients (Bohannon et al., 1988; Harris and Eng, 2004) and as a result, rehabilitation strategies often focus on this goal. Body-weight supported treadmill training (BWSTT) has been shown to be effective in improving post-stroke hemiparetic walking ability (Barbeau and Visintin, 2003; Hesse et al., 1995; Mulroy et al., 2010; Peurala et al., 2005; Plummer et al., 2007; Sullivan et al., 2007; Visintin et al., 1998). Previous studies have shown that most improvements in self-selected walking speed are maintained at a follow-up session three to six months after training has completed (Barbeau and Visintin, 2003; Peurala et al., 2005; Sullivan et al., 2007; Visintin et al., 1998). However, no study has identified the biomechanical quantities that predict long-term success in post-stroke rehabilitation. Quantities such as joint kinetics, step length, propulsion or daily step activity may be able to identify subjects who will be successful following post-stroke rehabilitation.

The ankle plantarflexors have been found to be the primary contributors to forward propulsion and critical to increasing walking speed in healthy walking (Liu et al., 2008; Neptune et al., 2008). However, paretic leg plantarflexor weakness is a primary impairment in post-stroke hemiparetic walking (e.g., Nadeau et al., 1999). Modeling and simulation studies of hemiparetic walking have also shown that the paretic leg plantarflexors (soleus and gastrocnemius) have reduced contributions to forward propulsion compared to control subjects walking at similar speeds (Peterson et al., 2010),

and that the reduced contributions limit functional walking status post-stroke (Hall et al., 2010). Other studies have shown that hemiparetic subjects who improve walking speed post-rehabilitation increase paretic leg ankle plantarflexor power (Mulroy et al., 2010; Parvataneni et al., 2007; Teixeira-Salmela et al., 2001).

Studies have also suggested that the paretic leg hip flexors may compensate for overall plantarflexor weakness in some hemiparetic subjects (Nadeau et al., 1999; Olney and Richards, 1996). In addition, hemiparetic subjects have increased hip flexor power output after rehabilitation with increased walking speed (Mulroy et al., 2010; Parvataneni et al., 2007; Teixeira-Salmela et al., 2001). Modeling and simulation studies of healthy walking have shown that the uniarticular hip flexors, iliacus and psoas, provide swing initiation together with gastrocnemius (Neptune et al., 2004; Neptune et al., 2008). Improved swing initiation provided by the paretic leg hip flexors will advance the paretic leg forward and increase the paretic leg step length.

In addition, subjects with hemiparesis typically generate asymmetric paretic and non-paretic leg anterior-posterior ground reaction forces (AP GRFs) during walking. A recent study revealed a positive correlation between propulsion symmetry and both hemiparetic severity and self-selected walking speed (Bowden et al., 2006), indicating that hemiparetic subjects who generate symmetric propulsion walk faster than subjects who generate asymmetric propulsion. Further, Bowden et al. (2006) showed that the paretic leg propulsive impulse (i.e., time integral of the paretic leg propulsive AP GRF) was positively correlated with hemiparetic severity and walking speed.

Similarly, persons with post-stroke hemiparesis walk with asymmetrical step lengths with the direction of asymmetry varying between subjects (e.g., Balasubramanian et al., 2007). Step length asymmetry has been shown to be negatively related to self-selected walking speed (Balasubramanian et al., 2007; Patterson et al., 2010) and

hemiparetic severity (Balasubramanian et al., 2007) and indicative of compensatory mechanisms in hemiparetic walking (Allen et al., 2010).

Daily step activity has been shown to be effective in quantitatively measuring levels of activity in the home and community in the hemiparetic population (Macko et al., 2002). A recent study showed that daily step activity is positively correlated with self-selected walking speed and an indicator of severity in hemiparetic subjects (Bowden et al., 2008).

The goal of this study was to identify potential biomechanical quantities that are predictive of success (as measured by self-selected walking speed) following post-stroke rehabilitation. Specifically, we analyzed joint moment impulses (i.e., time integral of the joint moment), step length asymmetry, AP GRF impulses (i.e., time integral of the AP GRF) and daily step activity at the end of rehabilitation. We expected that the paretic leg ankle plantarflexor moment impulse, the paretic leg hip flexor moment impulse, step length asymmetry, the paretic leg AP GRF impulse, and daily step activity to be important predictors of successful post-stroke rehabilitation, which we define as performance at the 6-month follow-up session relative to the post-training session. By identifying quantities that predict changes in self-selected walking speed over a 6-month follow-up period, this study will provide insight into the long-term effectiveness of BWSTT and help to identify subjects who will continue to improve after completing rehabilitation.

Methods

Subjects

A subset of 13 hemiparetic subjects (12 left hemiparesis; 10 men; age: mean = 59.0 years (SD = 11.1 years); time since stroke: mean = 18.2 months (SD = 14.4 months)) from a larger ongoing study at the Brain Rehabilitation Research Center at the Malcom Randall VA Medical Center (Gainesville, FL) participated in a 6-month follow-up study after completing a 12-week BWSTT intervention. Subject characteristics for the hemiparetic subjects are provided in Table B5 in Appendix B. Inclusion criteria for the hemiparetic subjects were: 1) at least 18 years of age, 2) stroke within past 6 months - 5 years, 3) residual paresis in the lower extremity (Fugl-Meyer LE motor score < 34), 4) ability to sit unsupported for 30 seconds, 5) ability to walk at least 10 feet with maximum 1 person assist, 6) self-selected 10-meter gait speed less than 0.8 m/s, 7) ability to follow a three step command. All subjects passed an exercise tolerance test (Yates et al., 2004) to verify their cardiovascular fitness prior to participation. Data from 21 age-matched healthy control subjects (4 men; age: mean = 65.2 years (SD = 9.6 years)) were also used in this study for comparison to the hemiparetic subjects. All subjects provided written informed consent approved by the Institutional Review Boards of the University of Florida and the University of Texas at Austin.

Training Intervention

Each hemiparetic subject participated in a 12-week BWSTT intervention consisting of training sessions three times a week. During each session, subjects participated in 20 minutes of walking using a BWSTT modality (Hesse et al., 1995; Plummer et al., 2007; Visintin et al., 1998) followed by 20 minutes of immediate

translation of skills acquired during treadmill walking to overground walking. During BWSTT, subjects wore a safety harness to protect against a loss of balance. Training began with 40% BWS and progressed as tolerated to no BWS. BWSTT took place at 2.0 – 3.0 mph with manual assistance provided by physical therapists at the hip and/or lower legs to approximate desired trunk, pelvis and lower limb kinematics and the spatio-temporal pattern of walking (Plummer et al., 2007).

Data Collection

Self-selected overground walking speed was measured as each hemiparetic subject completed two trials walking across a 4.3-meter GAITRite portable walkway system (CIR Systems, Inc., Clifton, NJ) at the pre-training, post-training and 6-month follow-up sessions. Each hemiparetic subject walked at their self-selected treadmill walking speed without the use of an assistive device on a split-belt instrumented treadmill (Tecmachine, Andrézieux Bouthéon, France) while data were collected for 30 seconds at the post-training session (Appendix C). Each control subject walked at 0.3, 0.6 and 0.9 m/s to provide speed-matched comparisons to the hemiparetic subjects. All subjects wore a safety harness mounted to the laboratory ceiling to protect against a loss of balance (no bodyweight was offloaded by the harness). A physical therapist was present for all data collection sessions. All data were collected using Vicon Workstation v4.5 software (Vicon Motion Capture Systems, Oxford, UK) and processed using Visual3D (C-motion, Inc., Germantown, MD). A 12-camera motion capture system (Vicon Motion Capture Systems, Oxford, UK) was used to determine bilateral kinematics from a modified Helen Hayes marker set with rigid clusters on the pelvis and each thigh, shank and foot segments. Marker trajectories and bilateral ground reaction force (GRF) data

were collected at 100 and 2000 Hz, respectively and were low-pass filtered with a fourth-order Butterworth filter with cutoff frequencies of 6 and 20 Hz, respectively. Daily step activity data were collected for eleven of the thirteen hemiparetic subjects post-training. Subjects wore a StepWatch^{TM} Activity Monitor (Orthocare Innovations, Washington, DC) for 4 days to calculate the average number of steps per day in the home and community.

Data Analysis

Intersegmental joint moments were calculated with a standard inverse dynamics analysis and normalized by body mass. GRF data were normalized by body weight. All data were time normalized to 100% of the paretic leg gait cycle for the hemiparetic subjects and to the right leg gait cycle for the control subjects. The propulsive phases of the paretic and non-paretic leg gait cycles for the hemiparetic subjects and for the right and left leg gait cycles for the control subjects were divided into late single-leg stance (i.e., second 50% of paretic single-leg stance) and pre-swing (i.e., double support region preceding paretic toe-off) regions. Sagittal plane hip (flexor positive), knee (extensor positive) and ankle (plantarflexor positive) joint moment impulses (i.e., time integral of the joint moment) and the AP GRF impulse (AP impulse) were calculated in each region. For the control subjects, the impulses for the right and left leg were averaged and data from all control subjects were averaged at each walking speed (0.3, 0.6 and 0.9 m/s). The impulses for the hemiparetic subjects were normalized by the average control data at matched speeds according to functional walking status (Perry et al., 1995) (Table 4.1). Step length symmetry (Paretic step ratio, PSR = paretic step length/(paretic + non-paretic step length)) and propulsion symmetry (Percent of Paretic Propulsion, PP = positive

paretic AP impulse/(positive paretic + non-paretic AP impulse)) were also calculated for each hemiparetic subject. To account for variations from symmetry (0.5), the absolute value of the deviation from 0.5 was calculated for the PSR and PP quantities. A speed ratio was calculated for each hemiparetic subject to indicate relative changes in overground self-selected walking speed from post-training to follow-up sessions (i.e., follow-up speed/post-training speed). Ratios between 0.9 and 1.1 were considered to indicate no relative change in speed between sessions. Pearson correlation coefficients were calculated between the speed ratios and all other quantities (joint moment and AP impulses, daily step activity, PSR and PP) at the post-training session with a significance level of 0.05. Statistical testing was conducted in SPSS 16.0 (SPSS, Inc., Chicago, IL).

Table 4.1. Joint moment and AP impulse data for the hemiparetic subjects were normalized by average control data at matched speeds based on functional walking status (Perry et al., 1995).

Functional walking status	Hemiparetic self-selected walking speed (m/s)	Control walking speed (m/s)
Household	< 0.4	0.3
Limited Community	0.4 – 0.8	0.6
Community	> 0.8	0.9

Results

The average self-selected walking speed for the hemiparetic subjects was 0.48 m/s (SD = 0.17 m/s), 0.67 m/s (SD = 0.23 m/s) and 0.68 m/s (SD = 0.28 m/s) at the pre-training, post-training and follow-up sessions, respectively (Table 4.2). Eight hemiparetic subjects had a clinically meaningful increase in self-selected walking speed from pre- to post-training (i.e., change in self-selected walking speed ≥ 0.16 m/s (Tilson

et al., 2010)) (Table 4.2). Four hemiparetic subjects increased walking speed (speed ratio > 1.1), seven hemiparetic subjects had no relative change in speed (0.9 ≤ speed ratio ≥ 1.1) and two hemiparetic subjects decreased walking speed (speed ratio < 0.9) from post-training to their 6-month follow-up sessions (Table 4.2). PSR was negatively related with the speed ratio ($p = 0.008$) (Table 4.3, Fig. 4.1). PP and daily step activity were not significantly related to the speed ratio, although daily step activity had a positive relationship and approached significance ($p = 0.052$) (Table 4.3, Fig. 4.1).

Table 4.2. Self-selected walking speed at the pre-training, post-training and follow-up sessions for the hemiparetic subjects. Speed ratios were calculated as follow-up/post-training speed. Subjects who had a change in self-selected walking speed from pre- to post-training that was determined to be clinically meaningful (change ≥ 0.16 m/s (Tilson et al., 2010)) are indicated by *.

Subject	Pre-training speed (m/s)	Post-training speed (m/s)	Follow-up speed (m/s)	Speed ratio
1	0.68	0.80	0.95	1.19
2	0.71	0.79	0.76	0.96
3	0.76	1.08*	1.06	0.99
4	0.35	0.64*	0.61	0.96
5	0.43	0.59*	0.49	0.83
6	0.39	1.00*	1.11	1.11
7	0.46	0.39	0.41	1.04
8	0.18	0.35*	0.24	0.68
9	0.29	0.31	0.31	0.99
10	0.50	0.75*	0.87	1.17
11	0.44	0.59	0.70	1.18
12	0.63	0.82*	0.80	0.98
13	0.43	0.59*	0.56	0.96
Average	0.48	0.67	0.68	
Standard Deviation	0.17	0.23	0.28	

Table 4.3. Correlations of post-training joint moment impulses, AP impulses, PSR, PP and daily step activity with the speed ratios (follow-up/post-training speed) for all hemiparetic subjects. Significant correlations are indicated in bold font ($p < 0.05$).

	r	p
PP	-0.401	0.087
PSR	**-0.648**	**0.008**
Daily step activity (steps per day)	0.516	0.052
Late single-limb stance region		
Joint moment impulses (N-m-msec/kg)		
Paretic leg hip	**0.492**	**0.044**
Paretic leg knee	**-0.548**	**0.026**
Paretic leg ankle	0.404	0.086
Non-paretic leg hip	0.316	0.146
Non-paretic leg knee	0.132	0.334
Non-paretic leg ankle	0.313	0.149
AP impulses (N-m-msec/BW)		
Paretic leg	0.373	0.104
Non-paretic leg	0.373	0.105
Pre-swing region		
Joint moment impulses (N-m-msec/kg)		
Paretic leg hip	0.44	0.066
Paretic leg knee	**-0.584**	**0.018**
Paretic leg ankle	0.4	0.088
Non-paretic leg hip	0.399	0.088
Non-paretic leg knee	-0.23	0.225
Non-paretic leg ankle	-0.008	0.49
AP impulses (N-m-msec/BW)		
Paretic leg	**0.571**	**0.021**
Non-paretic leg	-0.041	0.448

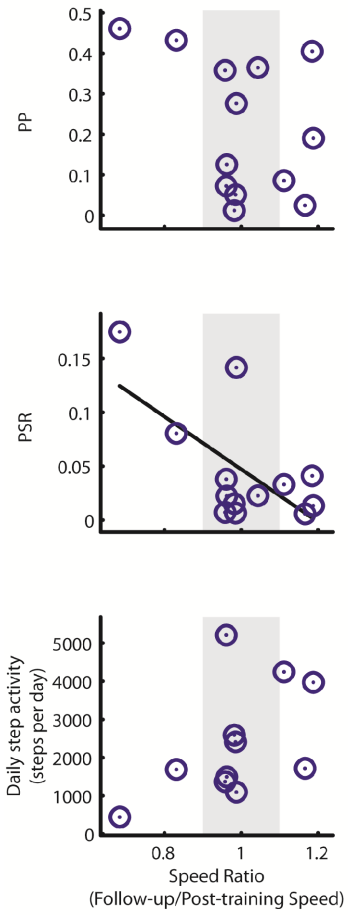

Figure 4.1. Post-training paretic propulsion symmetry (PP), step length symmetry (PSR) and daily step activity versus the speed ratio (follow-up/post-training speed) for all hemiparetic subjects. Shaded areas represent speed ratios between 0.9 and 1.1 and indicate no relative change in speed from post-training to follow-up sessions. The linear trend line is included for significant correlations.

Relationships with the speed ratio during the late single-limb stance region

The paretic leg hip (flexor positive) moment impulse was positively related ($p = 0.044$) and the paretic leg knee (extensor positive) moment impulse was negatively related ($p = 0.026$) to the speed ratio during late paretic leg single-limb stance (Table 4.3, Fig. 4.2). The paretic leg ankle (plantarflexor positive) and the non-paretic leg hip, knee

and ankle moment impulses were not significantly related to the speed ratio during late paretic and non-paretic single-limb stance regions, respectively. The paretic and non-paretic leg AP impulses were not significantly related to the speed ratio during the respective late single-limb stance regions.

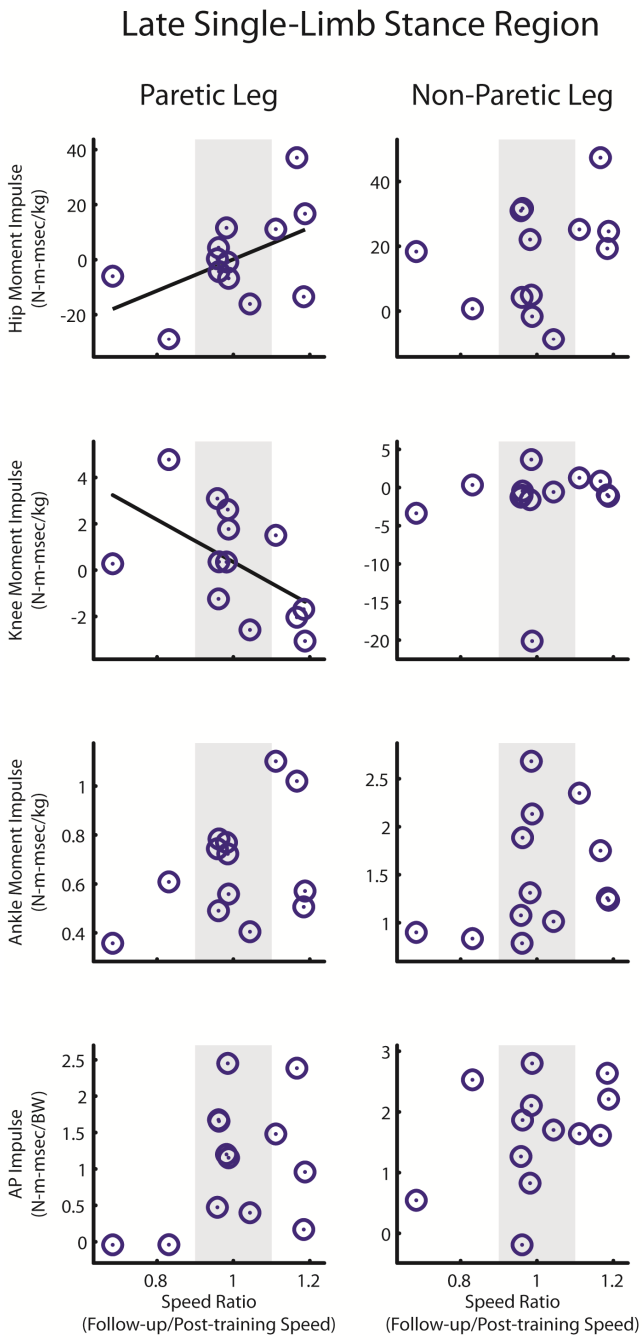

Figure 4.2. Post-training joint moment and anterior-posterior (AP) impulses versus speed ratio (follow-up/post-training speed) for all hemiparetic subjects during the late single-limb stance region. Shaded areas represent speed ratios between 0.9 and 1.1 and indicate no relative change in speed from post-training to follow-up sessions. The linear trend line is included for significant correlations.

Relationships with the speed ratio during the pre-swing region

The paretic leg knee moment impulse was negatively related to the speed ratio during paretic pre-swing ($p = 0.018$) (Table 4.3, Fig. 4.3). All other paretic and non-paretic leg joint moment impulses were not significantly related to the speed ratio during the respective pre-swing regions. The paretic leg AP impulse was positively related to the speed ratio during paretic pre-swing ($p = 0.021$) (Table 4.3, Fig. 4.3) while the non-paretic leg AP impulse was not significantly related to the speed ratio during non-paretic pre-swing.

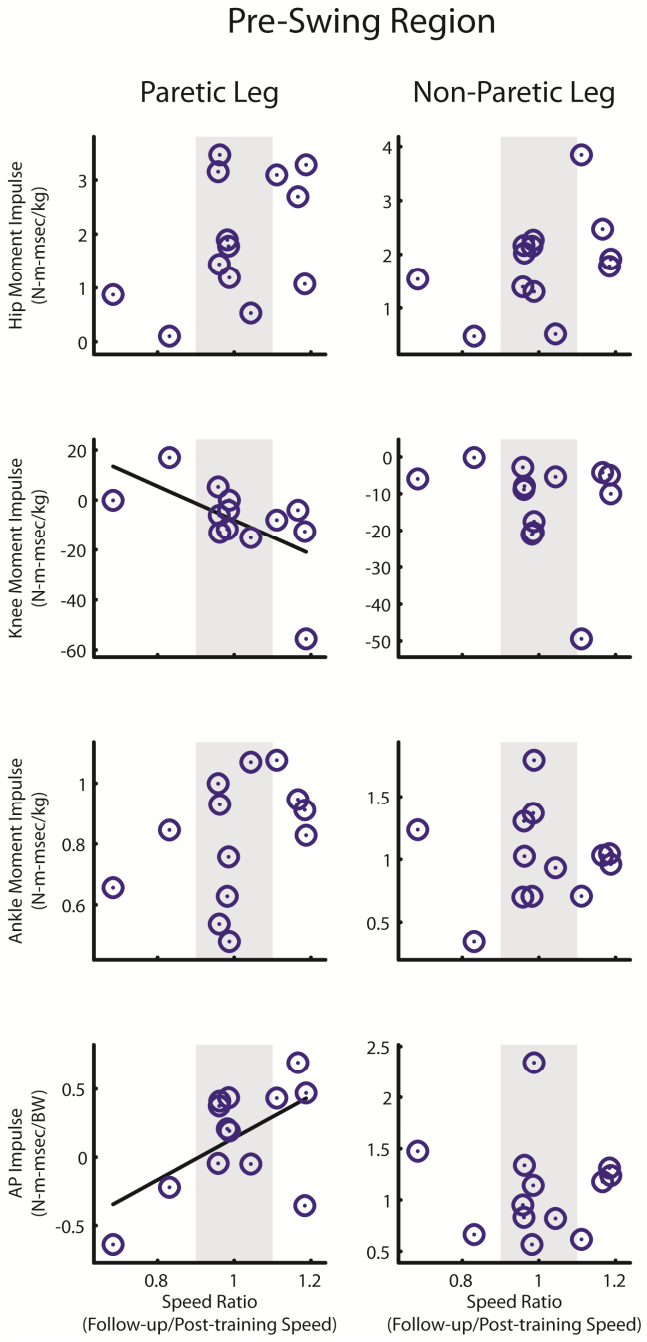

Figure 4.3. Post-training joint moment and anterior-posterior (AP) impulses versus speed ratio (follow-up/post-training speed) for all hemiparetic subjects during the pre-swing region. Shaded areas represent speed ratios between 0.9 and 1.1 and indicate no relative change in speed from post-training to follow-up sessions. The linear trend line is included for significant correlations.

Discussion

The goal of this study was to gain insight into the long-term effectiveness of post-stroke rehabilitation using BWSTT by seeking to understand the biomechanical characteristics of persons who maintain performance over a 6-month follow-up period. We used correlation analyses to determine if biomechanical quantities measured during the post-training session are predictive of success (as measured by self-selected walking speed) over a 6-month follow-up period following the completion of training. Most (8 out of 13) subjects had a clinically meaningful increase in self-selected walking speed (change $\geq$ 0.16 m/s) from pre- to post-training and had speed ratios that ranged from 0.68 to 1.17 (Table 4.2). The remaining subjects (5 out of 13) did not have a clinically meaningful increase in self-selected walking speed from pre- to post-training and had speed ratios that ranged from 0.96 to 1.19 (Table 4.2). Hemiparetic subjects who had similar speed ratios had changes in self-selected walking from pre- to post-training that were both clinically and not clinically meaningful, suggesting that the long-term effectiveness of rehabilitation training cannot be determined by changes in self-selected walking speed during training alone. The majority of subjects (11 out of 13) increased or did not change self-selected walking speed from post-training to follow-up sessions (Table 4.2), suggesting that the effects of BWSTT are maintained following training. This result is consistent with previous studies that showed subjects maintained self-selected walking speed three to six months after completion of BWSTT (Barbeau and Visintin, 2003; Peurala et al., 2005; Sullivan et al., 2007; Visintin et al., 1998).

Post-training PSR was a significant predictor of, and was negatively related to, the walking speed ratio (Table 4.3, Fig. 4.1). The negative relationship indicates that subjects with symmetric paretic and non-paretic steps had higher speed ratios than subjects with asymmetric step lengths. Previous studies have shown that hemiparetic

subjects with asymmetric step length have lower self-selected walking speed than subjects with symmetric step lengths (Balasubramanian et al., 2007; Patterson et al., 2010). Our results build upon this result and suggest that hemiparetic subjects who have more asymmetric step lengths post-training are more likely to reduce speed following training than subjects with symmetric step lengths. Post-training PSR was the strongest predictor of successful post-stroke rehabilitation ($r = -0.648$), suggesting that subjects who achieve symmetric step lengths at the end of training may have long-term success following rehabilitation.

Daily step activity measured at post-training had a positive relationship with the speed ratio that approached significance ($p = 0.052$) (Table 4.3, Fig 4.1), indicating that subjects who took more steps per day tended to increase walking speed from post-training to follow-up sessions. Daily step activity has been shown previously to serve as a quantitative measure of home and community walking performance (Bowden et al., 2008) and these results suggest that daily step activity may also identify subjects who are successful following post-stroke rehabilitation using BWSTT.

During late paretic leg single-limb stance, the post-training paretic leg hip moment impulse was positively related to the speed ratio (Table 4.3, Fig. 4.2), with hemiparetic subjects who generated a larger hip flexor moment impulse post-training than speed-matched controls increasing their speed following training. Previous studies have shown hemiparetic subjects use a hip strategy to compensate for reduced output from the paretic leg ankle plantarflexors (Nadeau et al., 1999) and that hemiparetic subjects increase hip flexor power output with increased speed during rehabilitation (Mulroy et al., 2010; Parvataneni et al., 2007; Teixeira-Salmela et al., 2001). The results of this study suggest that persons with post-stroke hemiparesis who increase output from

the paretic leg hip flexors relative to speed-matched controls may continue to improve walking speed following completion of rehabilitation training.

The paretic leg knee moment impulse at the post-training session was negatively related to the speed ratio in both late single-limb stance and pre-swing regions of the paretic leg gait cycle (Table 4.3, Figs. 4.2 and 4.3). Hemiparetic subjects who increased walking speed from post-training to follow-up sessions had post-training paretic leg knee moment impulses that were more extensor than speed-matched control subjects. The knee extensor moment has been shown to contribute to forward progression of the trunk segment from mid to late stance (Kepple et al., 1997) and therefore, hemiparetic subjects who have increased paretic leg knee extensor moments relative to speed-matched control subjects at the post-training may be compensating for reduced propulsion normally provided by the ankle plantarflexors in healthy walking (i.e., Neptune et al., 2001). Subjects who generated a paretic leg knee moment impulse that was more flexor than speed-matched controls at the post-training session decreased walking speed after training was completed. Increased knee flexion during mid to late stance may act to reduce paretic leg extension and therefore propulsion generation (Peterson et al., 2010). Therefore, subjects who generate increased knee extensor moment impulses relative to speed-matched control subjects post-training are likely generating increased paretic leg propulsion through improved leg extension. These results suggest that this knee extensor strategy may be indicative of success following rehabilitation.

During the paretic leg pre-swing region, the post-training paretic leg AP impulse was positively related to the speed ratio (Table 4.3, Fig. 4.3), suggesting that hemiparetic subjects who generated similar propulsion to control subjects post-training increased walking speed from post-training to follow-up sessions. Subjects who generated negative paretic leg propulsion (i.e., braking) relative to speed-matched controls post-training

decreased walking speed following training. Previous studies have shown that pre-swing propulsion generation by the paretic leg muscles is critical for improving walking speed post-stroke (Hall et al., 2010; Peterson et al., 2010). Thus, paretic leg propulsion generation in pre-swing appears to be a predictor of success following rehabilitation.

Although we expected that the paretic leg ankle moment impulse would be a predictor of success following rehabilitation, correlations between the paretic leg ankle moment impulse and the speed ratio during both the paretic leg late single-limb stance and pre-swing regions were not statistically significant, although both were positively related and approached significance (Table 4.3, Figs. 4.2 and 4.3). The hemiparetic subjects in this study had reduced paretic ankle plantarflexor joint moment impulses relative to control subjects at the post-training session, which is consistent with previous studies of post-stroke rehabilitation (Parvataneni et al., 2007; Teixeira-Salmela et al., 2001). To compensate for the reduced paretic leg ankle plantarflexor output, the hemiparetic subjects in the present study increased paretic leg hip flexion and knee extension moment impulses relative to speed-matched controls at the post-training session.

A potential limitation of this study is that we analyzed correlations between joint moment and AP impulses measured while subjects walked on a treadmill with the speed ratio generated from overground self-selected speed measurements. Although the hemiparetic subjects did generally walk slower on the treadmill than overground, we felt the use of overground speed measurements for the speed ratio was justified as it more closely represents the subjects' walking ability in the community. In addition, the use of an instrumented treadmill allowed for data collection to include a large number of gait cycles for a steady-state walking pattern, which is difficult to achieve with overground walking in the hemiparetic population.

Conclusion

This study analyzed joint moment impulses, AP impulses, step length symmetry, propulsion symmetry and daily step activity to identify variables that were predictors of success following completion of rehabilitation as measured by changes in self-selected walking speed from post-training to follow-up sessions. Improved step length symmetry, increased paretic leg hip flexor output in late paretic leg single-limb stance, increased paretic leg knee extensor output from mid to late paretic leg stance and increased paretic leg propulsion during pre-swing at the post-training session were all potential indicators of success following completion of rehabilitation. However, step length symmetry was the strongest predictor of success and therefore, step length symmetry may be an outcome measure that if targeted during rehabilitation could lead to long-term benefits for persons with post-stroke hemiparesis.

Chapter 5: Conclusion

The overall goal of this research was to investigate the underlying mechanisms that influence functional walking ability in post-stroke hemiparetic walking and understand the impact of post-stroke rehabilitation on walking ability in persons with post-stroke hemiparesis. This goal was accomplished with both simulation and experimental analyses of post-stroke hemiparetic walking. Hemiparetic subjects were analyzed before and after rehabilitation training with modeling and simulation techniques to identify the changes in muscle coordination (i.e., muscle force production and timing) that contribute to changes in functional walking status and walking speed. Experimental analyses were used to identify biomechanical predictors of success over a 6-month follow-up period after completion of post-stroke rehabilitation training. The results of this research provide insight into the factors that limit mobility for persons with post-stroke hemiparesis and provide rationale for developing effective post-stroke rehabilitation strategies.

Modeling and simulation analyses were used in Chapter 2 to determine muscle contributions to the walking subtasks of forward propulsion, swing initiation and power generation in the pre-swing phase of the gait cycle for hemiparetic subjects with different levels of functional walking status (i.e., community and limited community walkers) and speed-matched control subjects. The analyses showed that muscle contributions to the walking subtasks are indeed related to functional walking status in the hemiparetic subjects. Contributions from the paretic leg muscles (i.e., soleus, gastrocnemius and gluteus medius) to forward propulsion increased with improved functional walking status, with the non-paretic leg muscles (i.e. rectus femoris and vastii) compensating for reduced paretic leg propulsion in the limited community walker. Contributions to swing

initiation from both paretic (i.e. gastrocnemius, iliacus and psoas) and non-paretic leg muscles (i.e. hamstrings) also increased as functional walking status improved. Power generation was also an important indicator of functional walking status, with reduced paretic leg power generation limiting the paretic leg's contribution to forward propulsion and leg swing initiation. These results suggest that increasing contributions from the paretic leg muscles (i.e., ankle plantarflexors and hip flexors) and reducing contributions from the non-paretic leg muscles (i.e., hip and knee extensors) to the walking subtasks may be an effective rehabilitation strategy for improving post-stroke hemiparetic walking.

In Chapter 3, a large number of forward dynamics simulations of hemiparetic subjects walking pre- and post-locomotor training were developed to investigate changes in muscle contributions to propulsion (i.e., anterior-posterior acceleration of the body center-of-mass) with increased walking speed during rehabilitation. In order to investigate different strategies to increase walking speed, the hemiparetic subjects were divided into groups based on their pre-training propulsion symmetry. Subjects who generated little propulsion with their paretic leg at the pre-training session increased contributions to propulsion from non-paretic leg hamstrings and paretic leg gastrocnemius to improve walking speed. These results suggest that subjects who have low paretic leg propulsion pre-training may increase both paretic and non-paretic leg propulsion during post-stroke rehabilitation. In contrast, subjects who generated greater paretic leg propulsion pre-training relied on increased contributions from the paretic leg ankle plantarflexors (both soleus and gastrocnemius) to improve walking speed, suggesting that these subjects are more likely to increase paretic leg propulsion during rehabilitation. The results of this study revealed two primary strategies that hemiparetic

subjects use to increase walking speed and provide rationale for developing subject-specific post-stroke rehabilitation interventions that target specific muscle groups.

Experimental analyses were used in Chapter 4 to identify biomechanical variables, measured at the post-training session, that predict success (as measured by changes in self-selected walking speed) over a 6-month follow-up period following training. Several potential indicators of success following completion of rehabilitation emerged including improved step length symmetry, increased paretic leg hip flexor output in late paretic leg single-limb stance, increased paretic leg knee extensor output from mid to late paretic leg stance and increased paretic leg propulsion during pre-swing at the post-training session. The strongest predictor of success was step length symmetry suggesting that step length symmetry may be an outcome measure that if targeted during rehabilitation could lead to long-term benefits for persons with post-stroke hemiparesis.

Chapter 6: Future Work

The overall goal of this work was to investigate changes in post-stroke hemiparetic walking ability through both simulation and experimental analyses. The results provide rationale for developing effective post-stroke rehabilitation strategies and improving overall mobility in the hemiparetic population and can be expanded in several areas.

Individual muscle contributions to the walking subtasks of forward propulsion, swing initiation and power generation and to anterior-posterior body center-of-mass acceleration in post-stroke hemiparetic walking were identified in Chapters 2 and 3. Chapter 2 analyzed group average data of hemiparetic subjects with different levels of functional walking status (i.e., community and limited community walkers) and speed-matched control subjects. Because of the heterogeneity of the hemiparetic population, it is likely that a range of pre-swing deficits exist within the community and limited community walker groups. In addition, many hemiparetic subjects, classified as household walkers, have self-selected walking speeds less than 0.4 m/s and these subjects may have additional deficits in muscle coordination and muscle contributions to the walking subtasks. Future work should focus on developing subject-specific simulations of a large number of hemiparetic subjects with different levels of functional walking status to gain insight into the variability of the post-stroke hemiparetic population. Chapter 3 analyzed, for the first time, a large number of forward dynamics simulations of hemiparetic subjects to identify muscle contributions to anterior-posterior body center-of-mass acceleration. Other walking subtasks, such as body support and swing initiation, that impact overall mobility likely also change during rehabilitation. Future work should

investigate muscle contributions to other walking subtasks to further understand the impact of post-stroke rehabilitation on overall mobility.

Chapter 4 used experimental analyses to identify biomechanical predictors of successful post-stroke rehabilitation. Relationships between post-training joint kinetics and changes in self-selected walking speed over a 6-month follow-up period were investigated and provide important insight into variables that lead to long-term success in post-stroke rehabilitation. Future work using modeling and simulation analyses of these subjects could be used to understand specific changes in muscle coordination over a 6-month follow-up period following rehabilitation and provide additional insight into the effectiveness of rehabilitation strategies.

Appendix A: Musculotendon Regression Equations

To generate the forward dynamics simulations in Chapter 2, 515 parameters (6 excitation parameters for each of the 41 muscles per leg, 23 initial joint angular velocities) were optimized. A simulated annealing algorithm (Goffe et al., 1994) was used to determine the muscle excitations patterns (timing and magnitude) and the initial joint angular velocities that minimized the differences between the simulated and experimental kinematics and ground reaction forces (Fig. A1). Due to the high computational expense of this optimization problem, a large number of function calls (simulations) with the simulated annealing algorithm were required to converge to an optimal solution. Complex surfaces (e.g., wrapping surfaces) are needed to accurately replicate musculotendon moment arms and lengths in the musculoskeletal model (Fig. A2), but these complex surfaces are computationally expensive and increase simulation time. To reduce the computational expense and time to convergence, polynomial regression equations were fit to the muscle moment arm and musculotendon length data for each muscle in the musculoskeletal model. The regression equations maintained anatomically correct moment arms and allowed for removal of the patella segment from the musculoskeletal model and for removal of the planar knee model with prescribed motion, which was replaced with a revolute joint that is computationally more efficient.

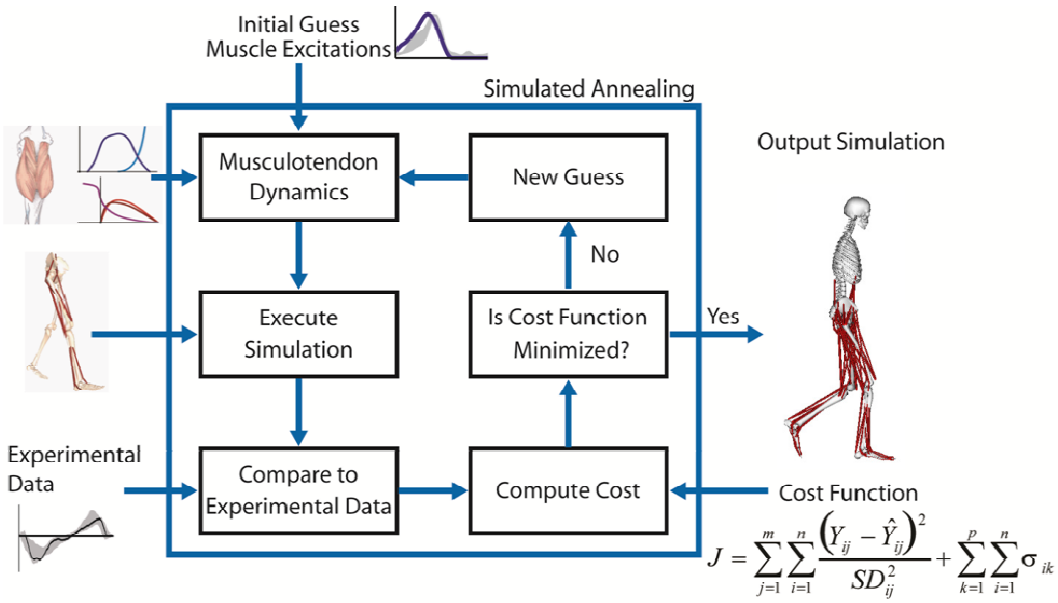

Figure A1. Schematic of a simulated annealing algorithm that determined the muscle excitation patterns that minimized differences between simulated and experimentally measured kinematics and ground reaction forces.

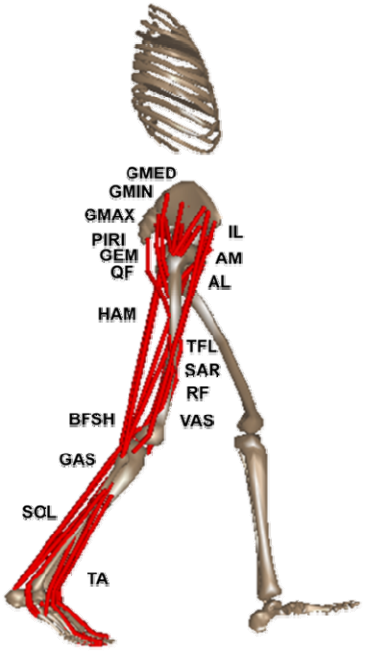

Figure A2. Bipedal 3D musculoskeletal model with 23 degrees-of-freedom and 43 individual musculotendon actuators, which were combined into 18 groups after analysis. Only muscles for the right leg are shown for clarity.

The regression equations were determined using a least-squares fitting method (Menegaldo et al., 2004). Musculotendon length and moment arm fitting equations can be expressed as:

$$F(Q_1,Q_2,Q_3,Q_4) = a_1 + a_2 f_1(Q_1,Q_2,Q_3,Q_4) + a_3 f_2(Q_1,Q_2,Q_3,Q_4) + \ldots + a_n f_{n-1}(Q_1,Q_2,Q_3,Q_4) \quad \text{(A1)}$$

where F represents a musculotendon's moment arms (r_i) or length (L_{mt}), Q_i is a generalized coordinate of the model, a_i are the coefficients to be determined, f_i are predetermined non-linear polynomial functions and n is a positive integer. In the lower extremity, every musculotendon actuator crosses one or two joints and its length and moment arm depends on the generalized coordinates (GC) of the corresponding joints. Because the maximum number of GCs for all muscles was four (biarticular muscles that cross the hip and knee), fitting equations with one to four GCs dependency were used (Table A1). The least-squares fitting method worked as follows: if k samples of data are available, matrix A and coefficient and function vectors **a** and **b** can be constructed as:

$$A = \begin{bmatrix} 1 & f_1(1) & \cdots & f_{n-1}(1) \\ \vdots & & \ddots & \vdots \\ 1 & f_1(k) & \cdots & f_{n-1}(k) \end{bmatrix} \quad \text{(A2)}$$

$$\mathbf{a} = [a_1, a_2, \ldots, a_n]^T \quad \text{(A3)}$$

$$\mathbf{b} = [F_1, F_2, \ldots, F_k]^T \quad \text{(A4)}$$

Using the least-squares normal equation, the coefficients (Tables A4, A5, A6, A7, A8 and A9) can be estimated from Equation A5 where $^+$ represents a pseudo-inverse matrix.

$$\mathbf{a} = (A^T A)^+ A^T \mathbf{b} \quad \text{(A5)}$$

Table A1. Fitting equations for musculotendon lengths (L_{mt}) and moment arms (R_i) depending on the number of generalized coordinates (GCs) from Menegaldo et al. (2004).

Number of GCs	Equation Number	Fitting Equations
4	1	$L_{mt}, R_1, R_2, R_3, R_4(Q_1, Q_2, Q_3, Q_4)=a_1+a_2Q_1+a_3Q_2+a_4Q_3+a_5Q_4+a_6Q_1^2+a_7Q_2^2+ \ldots a_8Q_3^2+a_9Q_4^2+a_{10}Q_1^3+a_{11}Q_2^3+a_{12}Q_3^3+a_{13}Q_4^3$
	2	$L_{mt}, R_1, R_2, R_3, R_4(Q_1, Q_2, Q_3, Q_4)=a_1+a_2Q_1+a_3Q_2+a_4Q_3+a_5Q_4+a_6Q_1Q_2+a_7Q_1Q_3+ \ldots a_8Q_1Q_4+a_9Q_2Q_3+a_{10}Q_2Q_4+a_{11}Q_3Q_4$
	3	$L_{mt}, R_1, R_2, R_3, R_4(Q_1, Q_2, Q_3, Q_4)=a_1+a_2Q_1+a_3Q_2+a_4Q_3+a_5Q_4$
	4	$L_{mt}, R_1, R_2, R_3, R_4(Q_1, Q_2, Q_3, Q_4)=a_1+a_2Q_1+a_3Q_2+a_4Q_3+a_5Q_4+a_6Q_1^2+a_7Q_2^2+ \ldots a_8Q_3^2+a_9Q_4^2+a_{10}Q_1Q_2Q_3Q_4$
3	1	$L_{mt}, R_1, R_2, R_3(Q_1, Q_2, Q_3)=a_1+a_2Q_1+a_3Q_2+a_4Q_3+a_5Q_1^2+a_6Q_2^2+a_7Q_3^2+a_8Q_1^3+a_9Q_2^3+a_{10}Q_3^3$
	2	$L_{mt}, R_1, R_2, R_3(Q_1, Q_2, Q_3)=a_1+a_2Q_1+a_3Q_2+a_4Q_3+a_5Q_1Q_2+a_6Q_1Q_3+a_7Q_2Q_3$
	3	$L_{mt}, R_1, R_2, R_3(Q_1, Q_2, Q_3)=a_1+a_2Q_1+a_3Q_2+a_4Q_3$
	4	$L_{mt}, R_1, R_2, R_3(Q_1, Q_2, Q_3)=a_1+a_2Q_1+a_3Q_2+a_4Q_3+a_5Q_1^2+a_6Q_2^2+a_7Q_3^2+a_8Q_1Q_2Q_3$
2	1	$L_{mt}, R_1, R_2(Q_1, Q_2)=a_1+a_2Q_1+a_3Q_2+a_4Q_1^2+a_5Q_2^2+a_6Q_1^3+a_7Q_2^3$
	2	$L_{mt}, R_1, R_2(Q_1, Q_2)=a_1+a_2Q_1+a_3Q_2+a_4Q_1Q_2$
	3	$L_{mt}, R_1, R_2(Q_1, Q_2)=a_1+a_2Q_1+a_3Q_2$
	4	$L_{mt}, R_1, R_2, R_3(Q_1, Q_2, Q_3)=a_1+a_2Q_1+a_3Q_2+a_4Q_1^2+a_5Q_2^2+a_6Q_1Q_2$
1	1	$L_{mt}, R_1(Q_1)=a_1+a_2Q_1+a_3Q_1^2+a_4Q_1^3$
	2	$L_{mt}, R_1(Q_1)=a_1+a_2Q_1+a_3Q_1^2$
	3	$L_{mt}, R_1(Q_1)=a_1+a_2Q_1$

MATLAB code provided by Menegaldo et al. (2004) were used to generate input files to SIMM to obtain data samples for regression fitting. All combinations of the GCs were sampled with 20 points across the range of motion expected for hemiparetic walking (Table A2). For muscles dependent on one, two, and three GCs, 20, 400, and 8000 points were generated, respectively. For muscles dependent on four GCs, data were sampled by 15 points such that 50,625 points were generated. Musculotendon actuators were placed into one of six groups based on the GCs spanned (Table A3).

Table A2. Generalized coordinates and the range of motion over which data were sampled to compute regression coefficients.

Generalized coordinate	Minimum (deg)	Maximum (deg)
Hip flexion (HF)	-40 extension	60 flexion
Hip abduction (HA)	-30 abduction	30 adduction
Hip rotation (HR)	-30 external	30 internal
Knee angle (KA)	-100 flexion	10 extension
Ankle angle (AA)	-30 plantar flexion	30 dorsiflexion
Subtalar angle (SA)	-40 eversion	40 inversion
Metatarsal angle (MA)	-5 flexion	40 extension

Table A3. Selected muscle groups according to dependence on the same generalized coordinates (GCs).

Group	Number of GCs dependent on	Muscle name
1	3: (HF, HA, HR)	Anterior, Middle and Posterior Gluteus Medius (GMED), Anterior, Middle and Posterior Gluteus Minimus (GMIN), Quadratus Femoris, Anterior, Middle and Posterior Gluteus Maximus (GMAX), Adductor Longus, Adductor Brevis, Pectineus, Tensor Fasciae Lata, Superior, Middle and Inferior Adductor Magnus (AM), Iliacus, Psoas, Piriformis, Gemellus
2	4: (HF, HA, HR, KA)	Semitendinosus, Semimembranosus, Biceps Femoris Long Head, Sartorius Gracilis, Rectus Femoris
3	1: (KA)	Vastus Medialis, Lateralis, and Intermedius, Biceps Femoris Short Head
4	3: (KA, AA, SA)	Medial and Lateral Gastrocnemius
5	2: (AA, SA)	Soleus, Tibialis Posterior, Tibialis Anterior, Peroneus Brevis, Peroneus Longus, Peroneus Tertius
6	3: (AA, SA, MA)	Flexor Digitorum Longus, Flexor Hallucis Longus, Extensor Digitorum Longus, Extensor Hallucis Longus

Table A4. Regression coefficients for Group 1 muscles dependent on 3 generalized coordinates to estimate musculotendon lengths (L_{mt}) and hip flexion, hip abduction, and hip rotation moment arms (R_{HF}, R_{HA}, R_{HR}) using the equations (Eq.) given in Table A1.

L_{mt}	**Anterior GMED**	**Middle GMED**	**Posterior GMED**	**Anterior GMIN**	**Middle GMIN**	**Posterior GMIN**	**Quadratus Femoris**
Eq.	2	2	2	1	1	1	1
a_1	0.12122	0.12938	0.10894	0.082448	0.082488	0.08617	0.069484
a_2	0.00024	0.000333	0.000383	3.4e-005	0.0001	0.000179	-6e-005
a_3	0.000807	0.000728	0.000584	0.00071	0.000705	0.00063	-0.000664
a_4	-0.000344	0.000113	0.000491	-0.000323	-0.000119	0.000135	0.000568
a_5	-2e-006	-2e-006	-3e-006	-1e-006	-1e-006	-1e-006	7e-006
a_6	-2e-006	0	-2e-006	-2e-006	-3e-006	-3e-006	-2e-006
a_7	2e-006	5e-006	3e-006	2e-006	2e-006	1e-006	-2e-006
a_8				0	0	0	0
a_9				0	0	0	0
a_{10}				0	0	0	0
R_{HF}							
Eq.	2	1	1	2	2	1	2
a_1	-0.012853	-0.022313	-0.023811	-0.001885	-0.005371	-0.010559	0.004048
a_2	0.000278	9.9e-005	-9.5e-005	0.000153	0.00015	8.8e-005	-0.000697
a_3	-1.6e-005	0.000124	0.000179	-1.1e-005	2e-005	5.8e-005	0.000264
a_4	-9.9e-005	1.7e-005	0.000108	-5.6e-005	-4.4e-005	5e-006	0.000143
a_5	0	3e-006	4e-006	0	-1e-006	1e-006	-1e-005
a_6	-1e-006	2e-006	1e-006	0	0	0	8e-006
a_7	4e-006	0	0	3e-006	3e-006	0	-6e-006
a_8		0	0			0	
a_9		0	0			0	

a_{10}		0	0			0	
R_{HA}							
Eq.	2	2	1	1	1	1	1
a_1	-0.0443	-0.041252	-0.035316	-0.042243	-0.042452	-0.038376	0.041961
a_2	-2.8e-005	0.000117	0.000206	-1.5e-005	1.8e-005	6.8e-005	0.000324
a_3	0.000148	0.000343	0.000397	0.000233	0.000302	0.000348	0.000191
a_4	-0.00039	-0.000293	-0.000151	-0.000238	-0.000156	-6.6e-005	1.8e-005
a_5	4e-006	3e-006	-1e-006	0	0	0	-5e-006
a_6	4e-006	3e-006	2e-006	3e-006	2e-006	2e-006	-3e-006
a_7	3e-006	3e-006	6e-006	6e-006	7e-006	6e-006	-3e-006
a_8			0	0	0	0	0
a_9			0	0	0	0	0
a_{10}			0	0	0	0	0
R_{HR}							
Eq.	2	2	2	2	2	2	2
a_1	0.019431	-0.006366	-0.027599	0.017645	0.006687	-0.007338	-0.034153
a_2	-0.000106	1.8e-005	0.00011	-5.5e-005	-4.5e-005	5e-006	0.000247
a_3	-0.000374	-0.000289	-0.00018	-0.000213	-0.000156	-9e-005	0.000104
a_4	-0.000159	-1.5e-005	2.6e-005	-0.000175	-0.000183	-7.1e-005	0.000186
a_5	4e-006	3e-006	1e-006	3e-006	3e-006	2e-006	-7e-006
a_6	-1e-006	0	0	-1e-006	0	1e-006	3e-006
a_7	1.2e-005	1.3e-005	1.2e-005	1.2e-005	1.3e-005	1.2e-005	-6e-006
L_{mt}	**Anterior GMAX**	**Middle GMAX**	**Posterior GMAX**	**Adductor Longus**	**Adductor Brevis**	**Pectineus**	**Tensor Fasciae Lata**
Eq.	2	1	2	2	2	2	1
a_1	0.19873	0.20962	0.23726	0.21714	0.13616	0.10276	0.53545
a_2	0.000689	0.000908	0.001146	-0.000531	-9.8e-005	-0.000354	-0.000581

a_3	0.000463	0.000173	-0.000778	-0.000998	-0.000973	-0.000509	0.000816
a_4	0.000359	0.000407	0.000504	-0.000121	-5.6e-005	-7.3e-005	-4.8e-005
a_5	-2e-006	-1e-006	6e-006	1e-006	2e-006	-1e-006	-7e-006
a_6	-2e-006	-1e-006	-1.5e-005	-1.7e-005	-1.5e-005	-9e-006	-6e-006
a_7	6e-006	4e-006	1e-006	0	0	-1e-006	3e-006
a_8		0					0
a_9		0					0
a_{10}		0					0

R_{HF}

Eq.	1	1	1	2	2	2	2
a_1	-0.045584	-0.055697	-0.073446	0.031423	0.008836	0.019807	0.031837
a_2	0.000173	0.000171	-0.000166	-0.000318	-0.00037	-8.7e-005	0.000721
a_3	0.000143	4.2e-005	-0.000276	9.4e-005	5.4e-005	0.00015	-4e-005
a_4	0.00012	0.000245	0.000921	0.000923	0.000811	0.000456	-0.000336
a_5	5e-006	5e-006	1.6e-005	-1.9e-005	-1.8e-005	-9e-006	2e-006
a_6	2e-006	0	-1e-006	0	-2e-006	3e-006	0
a_7	3e-006	9e-006	5e-006	-2e-006	-2e-006	0.019807	1.6e-005
a_8	0	0	0				
a_9	0	0	0				
a_{10}	0	0	0				

R_{HA}

Eq.	2	2	1	1	1	1	2
a_1	-0.026266	-0.010009	0.050122	0.066614	0.064746	0.032962	-0.04585
a_2	0.00013	4.4e-005	-0.000334	0.000152	6e-005	0.000206	-1.4e-005
a_3	0.000328	0.000124	-0.000145	0.000138	0.000305	0.000196	0.000708
a_4	-0.0004	-9e-005	-0.000105	1.8e-005	8e-006	5.4e-005	0.000216
a_5	4e-006	0	-4e-006	-9e-006	-1e-005	-4e-006	-4e-006
a_6	7e-006	3e-006	-9e-006	-8e-006	-5e-006	-3e-006	1.6e-005

a_7	2e-006	-1e-006	-3e-006	0	0	0	-1e-006
a_8			0	0	0	0	
a_9			0	0	0	0	
a_{10}			0	0	0	0	

R_{HR}							
Eq.	2	2	2	2	1	2	2
a_1	-0.019886	-0.021157	-0.027237	0.006721	0.003829	0.004081	0.006071
a_2	9.1e-005	0.000102	0.000797	0.000974	0.000963	0.000504	-0.000327
a_3	-0.000398	-9.5e-005	-1.5e-005	2.6e-005	1.5e-005	4.9e-005	0.00021
a_4	-0.000415	-0.000687	-0.00022	0.000155	0.00032	0.00023	-0.000322
a_5	7e-006	3e-006	-4e-006	-1e-006	1e-006	0	1.5e-005
a_6	7e-006	1.8e-005	1.6e-005	-7e-006	-1e-006	-4e-006	-7e-006
a_7	1.2e-005	4e-006	-5e-006	0	-1e-006	0	1e-005
a_8					0		
a_9					0		
a_{10}					0		

L_{mt}	**Superior AM**	**Middle AM**	**Inferior AM**	**Iliacus**	**Psoas**	**Piriformis**	**Gemellus**
Eq.	2	2	2	1	1	1	1
a_1	0.12026	0.1998	0.34267	0.20596	0.2571	0.13634	0.064391
a_2	0.000145	0.000382	0.000271	-0.000554	-0.000528	0.000158	-2.1e-005
a_3	-0.001109	-0.000993	-0.000864	3.3e-005	-7.8e-005	0.000317	-0.000198
a_4	5.7e-005	2.8e-005	-1e-005	-6.6e-005	-8.3e-005	0.000491	0.000542
a_5	3e-006	5e-006	4e-006	-3e-006	-3e-006	1e-006	1e-006
a_6	-1.4e-005	-1.4e-005	-1.5e-005	-1e-006	-1e-006	-2e-006	-1e-006
a_7	1e-006	2e-006	2e-006	2e-006	2e-006	-2e-006	-2e-006
a_8				0	0	0	0
a_9				0	0	0	0
a_{10}				0	0	0	0

R_{HF}

Eq.	2	2	2	1	1	1	2
a_1	0.000331	-0.011725	-0.006084	0.03368	0.031963	-0.009111	0.00122
a_2	-0.000761	-0.000807	-0.000823	0.000328	0.0003	-0.000101	-0.00016
a_3	6.2e-005	-3.9e-005	-1.2e-005	-1.1e-005	1.3e-005	7.7e-005	4.4e-005
a_4	0.000748	0.0008	0.000851	2.2e-005	0.000153	6.6e-005	-3e-006
a_5	-2.1e-005	-1.8e-005	-1.8e-005	-2e-006	-2e-006	2e-006	-1e-006
a_6	-3e-006	-5e-006	-4e-006	0	0	0	2e-006
a_7	-8e-006	-1.1e-005	-1.2e-005	-6e-006	-6e-006	0	-1e-006
a_8				0	0	0	
a_9				0	0	0	
a_{10}				0	0	0	

R_{HA}

Eq.	1	1	1	2	2	1	2
a_1	0.07565	0.067832	0.059159	-0.001735	0.004133	-0.019729	0.010637
a_2	-1.3e-005	-0.000129	-5.9e-005	-1.1e-005	1.7e-005	9.1e-005	3.8e-005
a_3	9e-005	-0.000514	-0.000812	0.000118	0.000108	0.000268	0.000156
a_4	-7.1e-005	-0.000134	-0.000136	1.5e-005	1.9e-005	2e-005	-3.9e-005
a_5	-1.3e-005	-1e-005	-1e-005	1e-006	1e-006	0	-1e-006
a_6	-9e-006	-1.2e-005	-1e-005	3e-006	2e-006	1e-006	-1e-006
a_7	-2e-006	-1e-006	0	0	0	3e-006	-1e-006
a_8	0	0	0			0	
a_9	0	0	0			0	
a_{10}	0	0	0			0	

R_{HR}

Eq.	2	2	2	2	2	2	1
a_1	-0.003207	-0.001561	0.000586	0.003383	0.002983	-0.027926	-0.031936
a_2	0.000791	0.000802	0.000856	9e-006	0.000116	7.1e-005	-3e-006

a_3	3e-006	-1.5e-005	-5e-006	1.4e-005	1.7e-005	4e-006	-4.2e-005
a_4	0.000335	0.000143	-3.6e-005	-7.5e-005	-6e-005	0.000183	0.000261
a_5	-7e-006	-1.2e-005	-1.3e-005	2e-006	2e-006	0	1e-006
a_6	1e-006	4e-006	3e-006	-1.2e-005	-1.1e-005	0	0
a_7	-3e-006	-2e-006	0.000586	1e-006	0	5e-006	2e-006
a_8							0
a_9							0
a_{10}							0

Table A5. Regression coefficients for Group 2 muscles dependent on 4 generalized coordinates to estimate musculotendon lengths (L_{mt}) and hip flexion, hip abduction, hip rotation, and knee angle moment arms (R_{HF}, R_{HA}, R_{HR}, R_{KA}) using the equations (Eq.) given in Table A1.

L_{mt}	**Semi-membranosus**	**Semi-tendinosus**	**Biceps Femoris Long Head**	**Sartorius**	**Gracilis**	**Rectus Femoris**
Eq.	1	1	1	4	2	4
a_1	0.41514	0.4642	13	0.56825	0.45159	0.40992
a_2	0.000794	0.000933	0.44096	-0.00072	0.000131	-0.000648
a_3	-0.000197	-0.000335	0.000873	0.000402	-0.00082	0.00018
a_4	-4.5e-005	-6.5e-005	-0.000325	0.000194	8e-005	5.1e-005
a_5	0.00044	0.000731	9.2e-005	4e-005	0.00064	-0.000809
a_6	6e-006	7e-006	0.000219	-7e-006	1e-006	-3e-006
a_7	5e-006	6e-006	5e-006	-8e-006	-1.6e-05	-4e-006
a_8	0	0	4e-006	0	0	2e-006
a_9	-8e-006	-5e-006	0	-3e-006	1e-006	-3e-006
a_{10}	0	0	-1.1e-005	0	0	0.40992
a_{11}	0	0	0			
a_{12}	0	0	0			
a_{13}	0	0	0			
R_{HF}						
Eq.	4	4	4	2	2	1
a_1	-0.049162	-0.056283	-0.054583	0.039583	0.001715	0.042149
a_2	-0.000625	-0.000762	-0.000592	0.000821	-0.00086	0.00053
a_3	-2.4e-005	-4.8e-005	-3.7e-005	-3.6e-005	9.8e-005	4e-005
a_4	0.000199	0.000332	0.000251	-0.00051	0.000834	-0.000183
a_5	-5.8e-005	-4.2e-005	-6.3e-005	0	-1.4e-05	2.1e-005
a_6	9e-006	1.1e-005	9e-006	9e-006	-1.8e-05	-5e-006
a_7	1e-006	1e-006	1e-006	-1e-006	-2e-006	-1e-006
a_8	7e-006	8e-006	7e-006	0	0	-5e-006
a_9	0	-1e-006	0	1.5e-005	-1.3e-05	0
a_{10}	0	0	0	0	0	0
a_{11}				0	0	0
a_{12}						0
a_{13}						0
R_{HA}						
Eq.	2	2	2	2	4	2
a_1	0.010981	0.018599	0.017679	-0.02316	0.056692	-0.010448

a_2	-3.8e-005	-5.3e-005	-6.4e-005	4.5e-005	0.000103	4.5e-005
a_3	-0.000564	-0.000719	-0.000489	0.000906	-0.00085	0.000484
a_4	6.3e-005	0.000113	3.6e-005	1.5e-005	-5.2e-005	7.5e-005
a_5	3e-006	2e-006	-7e-006	0	-6e-006	1e-006
a_6	1e-006	2e-006	1e-006	-1e-006	-9e-006	-2e-006
a_7	-9e-006	-1.2e-005	-9e-006	1.5e-005	-1e-005	9e-006
a_8	0	0	0	0	0	0
a_9	0	0	0	1e-006	0	1e-006
a_{10}	0	0	0	0	0	0
a_{11}	-1e-006	0	-1e-006	0		0

R_{HR}

Eq.	2	2	2	2	2	2
a_1	0.000767	-0.000225	-0.005803	-0.00552	-0.00441	-0.001448
a_2	0.000206	0.000348	0.000255	-0.00053	0.000865	-0.000181
a_3	6.2e-005	0.000112	3.5e-005	1.4e-005	7.1e-005	7.4e-005
a_4	-9.9e-005	-0.00017	-3.8e-005	7.2e-005	-6.1e-05	-9e-005
a_5	8e-006	-9e-006	3.9e-005	0	1.4e-005	-9e-006
a_6	-1e-005	-1.2e-005	-9e-006	1.5e-005	-1.3e-05	9e-006
a_7	1.4e-005	1.6e-005	1.5e-005	-1.2e-005	1e-006	-1e-005
a_8	0	0	0	0	0	0
a_9	0	0	-1e-006	-3e-006	0	0
a_{10}	-1e-006	0	-1e-006	0	0	0
a_{11}	1e-006	0	2e-006	0	0	0

R_{KA}

Eq.	1	4	1	1	1	1
a_1	-0.026321	-0.042167	-0.014082	-0.00153	-0.02467	0.042061
a_2	-2.5e-005	1.6e-005	-5.3e-005	0	-1.3e-05	3e-005
a_3	0	3e-006	-1.2e-005	0	-2e-006	3e-006
a_4	7e-006	-9e-006	3.8e-005	0	1.1e-005	-1.2e-005
a_5	0.000809	0.000505	0.001043	0.000355	0.000539	-0.000429
a_6	0	0	1e-006	0	0	0
a_7	0	0	0	0	0	0
a_8	0	0	1e-006	0	0	0
a_9	3e-006	8e-006	1e-006	0	4e-006	-2e-005
a_{10}	0	0	0	0	0	0
a_{11}	0		0	0	0	0
a_{12}	0		0	0	0	0
a_{13}	0		0	0	0	0

Table A6. Regression coefficients for Group 3 muscles dependent on 1 generalized coordinate to estimate musculotendon lengths (L_{mt}) and knee angle moment arms (R_{KA}) using the equations (Eq.) given in Table A1.

L_{mt}	**Vastus Medialis**	**Vastus Lateralis**	**Vastus Intermedius**	**Biceps Femoris Short Head**
Eq.	2	1	1	1
a_1	0.17273	0.20073	0.18251	0.25884
a_2	-0.000679	-0.000656	-0.000756	6.5e-005
a_3	-1e-006	-1e-006	-3e-006	-9e-006
a_4		0	0	0
R_{KA}				
Eq.	1	1	1	1
a_1	0.036804	0.033036	0.039485	-0.004308
a_2	-0.000212	-0.0005	-0.000163	0.000905
a_3	-1.1e-005	-1.7e-005	-1.2e-005	0
a_4	0	0	0	0

Table A7. Regression coefficients for Group 4 muscles dependent on 3 generalized coordinates to estimate musculotendon lengths (L_{mt}) and knee, ankle and subtalar angle moment arms (R_{KA}, R_{AA}, R_{SA}) using the equations (Eq.) given in Table A1.

L_{mt}	**Medial Gastrocnemius**	**Lateral Gastrocnemius**
Eq.	1	1
a_1	0.45032	0.44749
a_2	0.000182	0.000219
a_3	0.000709	0.000726
a_4	-2.6e-005	-7.7e-005
a_5	0	0
a_6	-2e-006	-2e-006
a_7	2e-006	2e-006
a_8	0	0
a_9	0	0
a_{10}	0	0
R_{KA}		
Eq.	3	3
a_1	-0.014631	-0.016594
a_2	-0.000169	-0.000232
a_3	0	0
a_4	0	0
R_{AA}		
Eq.	1	1
a_1	-0.041733	-0.042777
a_2	0	0
a_3	0.000205	0.00022
a_4	5.1e-005	4.6e-005
a_5	0	0
a_6	6e-006	6e-006
a_7	2e-006	2e-006
a_8	0	0
a_9	0	0
a_{10}	0	0
R_{SA}		
Eq.	2	2
a_1	0.001373	0.004013
a_2	0	0

a_3	4.6e-005	4.2e-005
a_4	-0.00028	-0.000276
a_5	0	0
a_6	0	0
a_7	4e-006	4e-006

Table A8. Regression coefficients for Group 5 muscles dependent on 2 generalized coordinates to estimate musculotendon lengths (L_{mt}) and ankle and subtalar angle moment arms (R_{AA}, R_{SA}) using the equations (Eq.) given in Table A1.

L_{mt}	**Soleus**	**Tibialis Posterior**	**Tibialis Anterior**	**Peroneus Brevis**	**Peroneus Longus**	**Peroneus Tertius**
Eq.	4	4	4	2	1	4
a_1	0.29079	0.34528	0.30357	0.2106	0.39533	0.17804
a_2	0.000681	0.000193	-0.000668	6.9e-005	0.000157	-0.0004
a_3	-6e-005	-0.00031	-0.000222	0.000459	0.000483	0.0003
a_4	-2e-006	-1e-006	-1e-006	1e-006	0	0
a_5	2e-006	1e-006	-1e-006		0	1e-006
a_6	-1e-006	1e-006	1e-006		0	-6e-006
a_7					0	
R_{AA}						
Eq.	4	4	4	4	4	4
a_1	-0.041235	-0.011592	0.042213	-0.004837	-0.009827	0.026731
a_2	0.000257	9e-005	7.4e-005	-2.3e-005	-1.5e-005	-4.8e-005
a_3	3.7e-005	-8e-005	-3.8e-005	-7.6e-005	-5.4e-005	0.000333
a_4	5e-006	1e-006	-5e-006	0	2e-006	-3e-006
a_5	2e-006	1e-006	-5e-006	1e-006	2e-006	-5e-006
a_6	-2e-006	-3e-006	2e-006	7e-006	7e-006	8e-006
R_{SA}						
Eq.	4	1	4	1	1	4
a_1	0.003966	0.019908	0.012948	-0.031675	-0.030373	-0.019456
a_2	3.5e-005	-8e-005	-5.4e-005	-0.000115	-6.4e-005	0.000334
a_3	-0.000264	-7.9e-005	0.000105	0.000219	0.000191	-8.3e-005
a_4	-1e-006	-2e-006	1e-006	5e-006	5e-006	4e-006
a_5	-1e-006	-4e-006	-2e-006	1.1e-005	9e-006	3e-006
a_6	4e-006	0	-1e-005	0	0	-1.1e-005
a_7		0		0	0	

Table A9. Regression coefficients for Group 6 muscles dependent on 3 generalized coordinates to estimate musculotendon lengths (L_{mt}) and ankle, subtalar and metatarsal angle moment arms (R_{AA}, R_{SA}, R_{MA}) using the equations (Eq.) given in Table A1.

L_{mt}	**Flexor Digitorum Longus**	**Flexor Hallucis Longus**	**Extensor Digitorum Longus**	**Extensor Hallucis Longus**
Eq.	3	3	4	4
a_1	0.43041	0.41534	0.45388	0.42225
a_2	-0.000424	-0.000352	0.000238	-9.8e-005
a_3	5.6e-005	5.9e-005	-6.4e-005	-7.7e-005
a_4	0.000246	0.000362	-0.000825	-0.000844
a_5			-1e-006	-1e-006
a_6			0	0
a_7			0	-1e-006
a_8			0	0
R_{AA}				
Eq.	1	1	3	3
a_1	-0.01301	-0.018401	0.035077	0.035927
a_2	-0.000125	-0.000111	0.000135	-8.7e-005
a_3	0	0	0	0
a_4	8.5e-005	9.4e-005	-2.4e-005	2.8e-005
a_5	0	1e-006		
a_6	0	0		
a_7	3e-006	3e-006		
a_8	0	0		
a_9	0	0		
a_{10}	0	0		
R_{SA}				
Eq.	4	4	3	1
a_1	0.021011	0.017527	-0.012012	0.006088
a_2	-3.1e-005	-5.1e-005	5.9e-005	5.8e-005
a_3	0	0	0	0
a_4	-2.3e-005	-3.1e-005	0.00012	-9.3e-005
a_5	-6e-006	-5e-006		-1e-006
a_6	0	0		0
a_7	-3e-006	-2e-006		-1e-006
a_8	0	0		0
a_9				0
a_{10}				0

R_{MA}				
Eq.	4	3	4	4
a_1	-0.005695	-0.005935	0.006546	0.007954
a_2	0	0	0	0
a_3	2.8e-005	-1e-006	2.4e-005	3.5e-005
a_4	0	0	0	0
a_5	0		0	0
a_6	0		0	0
a_7	0		0	0
a_8	0		0	0

Appendix B: Subject Characteristics

Subject characteristics for the hemiparetic and control subjects in Chapter 2 are provided in Tables B1, B2 and B3. Subject characteristics for the hemiparetic subjects in Chapter 3 are provided in Table B4. Subject characteristics for the hemiparetic subjects in Chapter 4 are provided in Table B5.

Table B1. Subject characteristics for the community hemiparetic subjects who were included in the study in Chapter 2.

	Age (years)	**Gender**	**Paretic Side**	**Time Since Stroke (months)**
1	60	M	L	101
2	57	M	L	39
3	64	M	R	19
4	67	M	L	23
5	58	M	R	27
Average	**61.2**	**-**	**-**	**41.8**
Standard Deviation	**4.2**	**-**	**-**	**33.9**

Table B2. Subject characteristics for the limited community hemiparetic subjects who were included in the study in Chapter 2.

	Age (years)	Gender	Paretic Side	Time Since Stroke (months)
1	49	M	R	95
2	45	F	R	11
3	62	M	R	116
4	63	M	L	114
5	82	M	R	29
6	60	M	R	58
7	76	F	R	7
8	53	M	L	25
9	54	F	L	76
10	40	F	R	43
11	72	M	L	64
12	46	F	L	95
13	72	M	R	86
14	60	M	R	27
15	57	M	R	26
16	44	M	R	301
17	67	M	L	17
18	49	F	R	16
19	64	F	L	58
20	71	F	R	23
21	62	M	L	47
Average	**59.4**	**-**	**-**	**63.8**
Standard Deviation	**11.5**	**-**	**-**	**65.9**

Table B3. Subject characteristics for the control subjects who were included in the study in Chapter 2. Control subjects walked at fixed speeds of 0.6 and 0.9 m/s for comparison with the hemiparetic subjects.

	Age (years)	Gender
1	70	M
2	58	F
3	54	F
4	54	F
5	62	F
6	59	F
7	51	F
8	55	M
9	52	F
10	78	F
11	61	F
12	83	F
13	71	F
14	80	F
15	79	F
16	71	M
17	68	F
18	59	M
19	59	F
Average	**65.2**	**-**
Standard Deviation	**9.6**	**-**

Table B4. Subject characteristics for the hemiparetic subjects who were included in the study in Chapter 3.

	Age (years)	Gender	Paretic Side	Time Since Stroke (months)
1	45	F	L	11
2	83	M	R	46
3	64	M	L	12
4	74	M	R	22
5	52	M	L	8
6	44	M	L	10
7	55	M	R	21
8	62	M	L	56
9	57	M	R	13
10	62	F	L	17
Average	**59.8**	**-**	**-**	**21.6**
Standard Deviation	**12.1**	**-**	**-**	**16.3**

Table B5. Subject characteristics for the hemiparetic subjects who were included in the study in Chapter 4.

	Age (years)	Gender	Paretic Side	Time Since Stroke (months)
1	44	F	L	7
2	48	M	L	59
3	56	M	L	12
4	61	F	L	9
5	64	M	L	12
6	57	M	R	32
7	71	M	L	9
8	83	M	L	18
9	52	M	L	8
10	44	M	L	10
11	57	M	L	27
12	68	M	L	17
13	62	F	L	17
Average	**59.0**	**-**	**-**	**18.2**
Standard Deviation	**11.1**	**-**	**-**	**14.4**

Appendix C: Experimental Data Collection Setup

Experimental data for all studies were collected at the VA Brain Rehabilitation Research Center at the Malcom Randall VA Medical Center (Gainesville, FL). Kinematic, ground reaction force and electromyographic data were collected while the subjects walked on a split-belt instrumented treadmill (Fig. C1).

Figure C1. A representative post-stroke hemiparetic subject walking on a split-belt instrumented treadmill while experimental data were collected. Reflective markers were placed on the head (top, left and right temple and back), trunk (C7, T10, clavicle, sternum and right scapula), and arms (left and right shoulder, elbow and wrist). Clusters of reflective markers were attached to the pelvis and left and right thigh, shank and foot segments.

Appendix D: Simulated and Experimental Data Comparisons

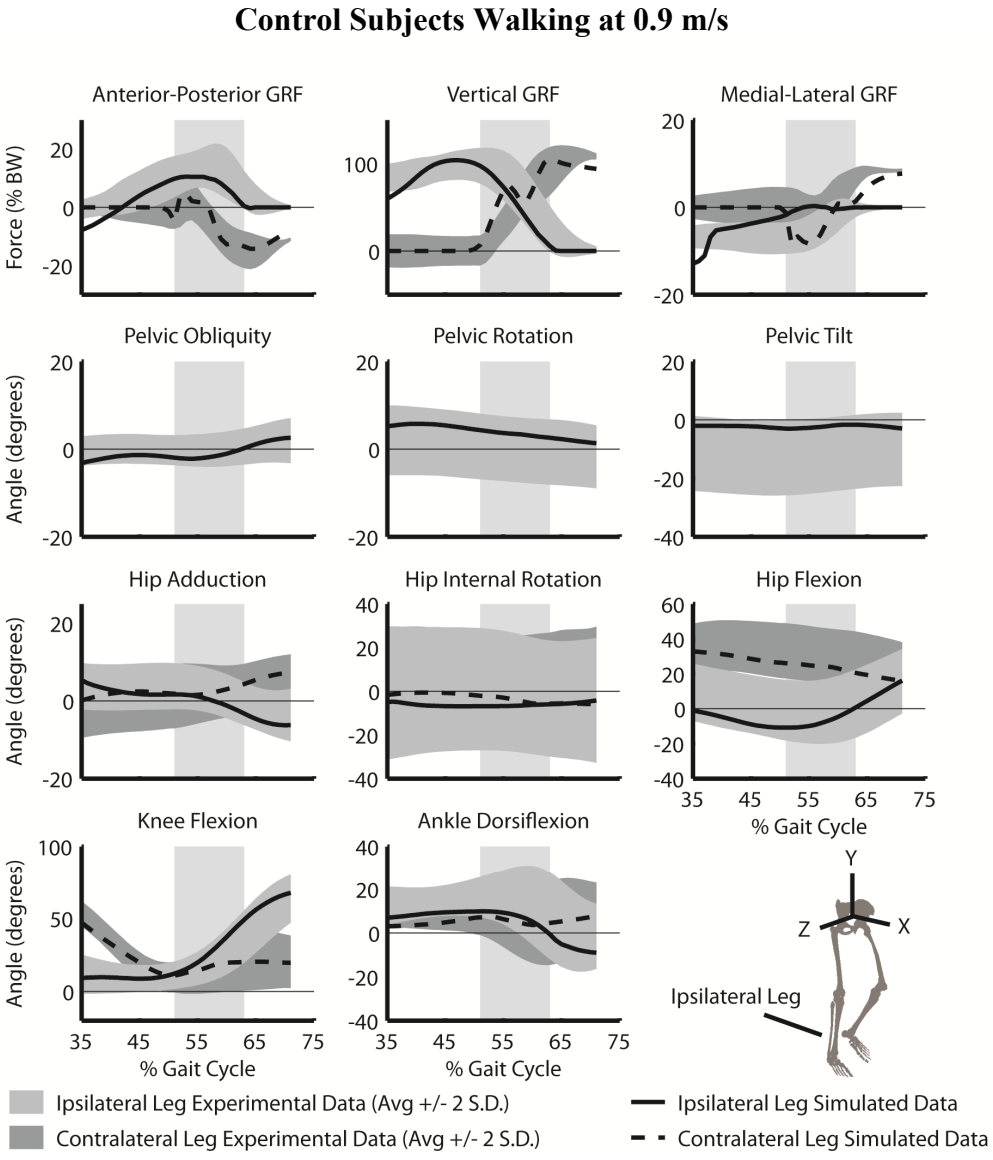

Figure D1. Simulated and experimental ground reaction force (GRF) and kinematic data for the control subjects walking at 0.9 m/s who were included in the study in Chapter 2. Experimental data are normalized to the ipsilateral leg gait cycle and shown as the average +/- 2 standard deviations (S.D.). Positive joint angles correspond to plot subtitles. Positive pelvic obliquity, rotation and tilt correspond to positive rotations about the X, Y and Z pelvis segment axes, respectively (see bottom right). The shaded vertical bar indicates the ipsilateral leg pre-swing region.

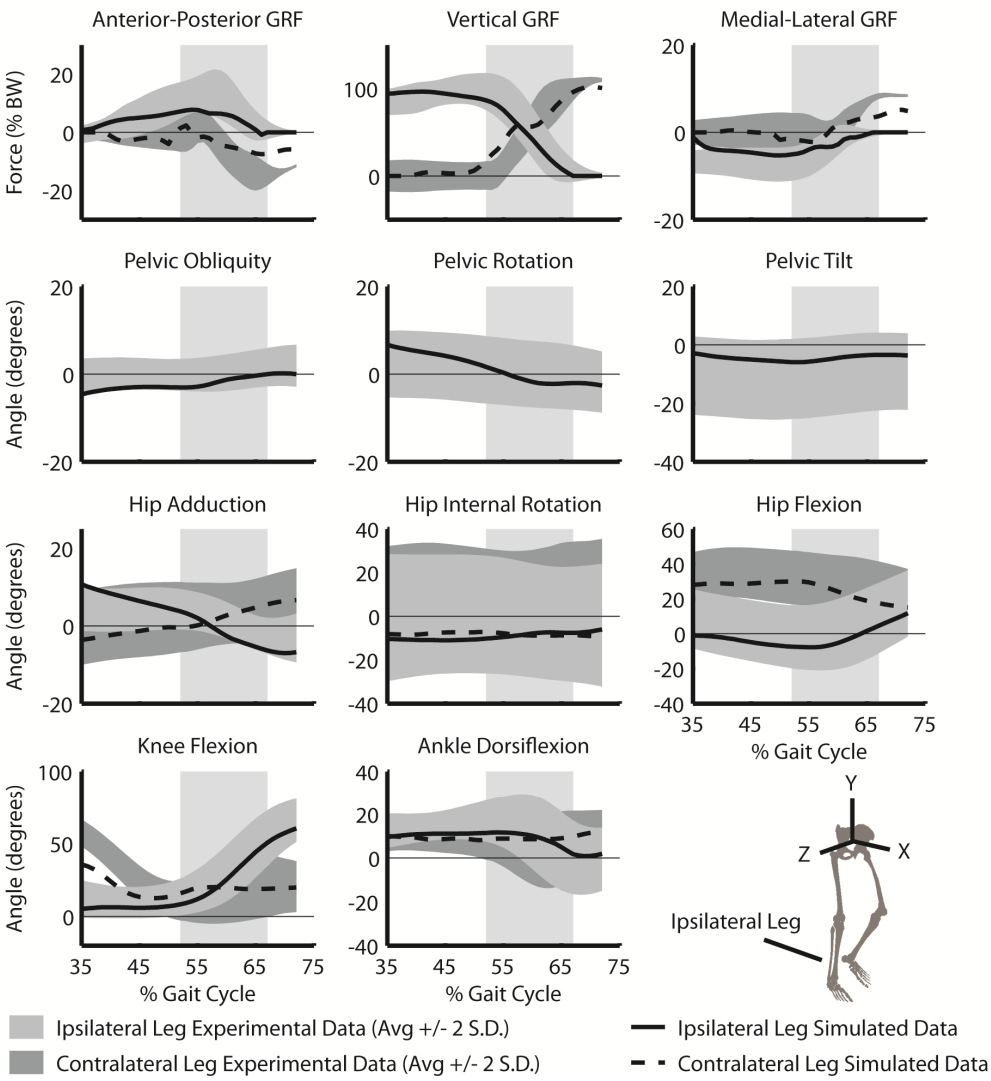

Figure D2. Simulated and experimental ground reaction force (GRF) and kinematic data for the control subjects walking at 0.6 m/s who were included in the study in Chapter 2. Experimental data are normalized to the ipsilateral leg gait cycle and shown as the average +/- 2 standard deviations (S.D.). Positive joint angles correspond to plot subtitles. Positive pelvic obliquity, rotation and tilt correspond to positive rotations about the X, Y and Z pelvis segment axes, respectively (see bottom right). The shaded vertical bar indicates the ipsilateral leg pre-swing region.

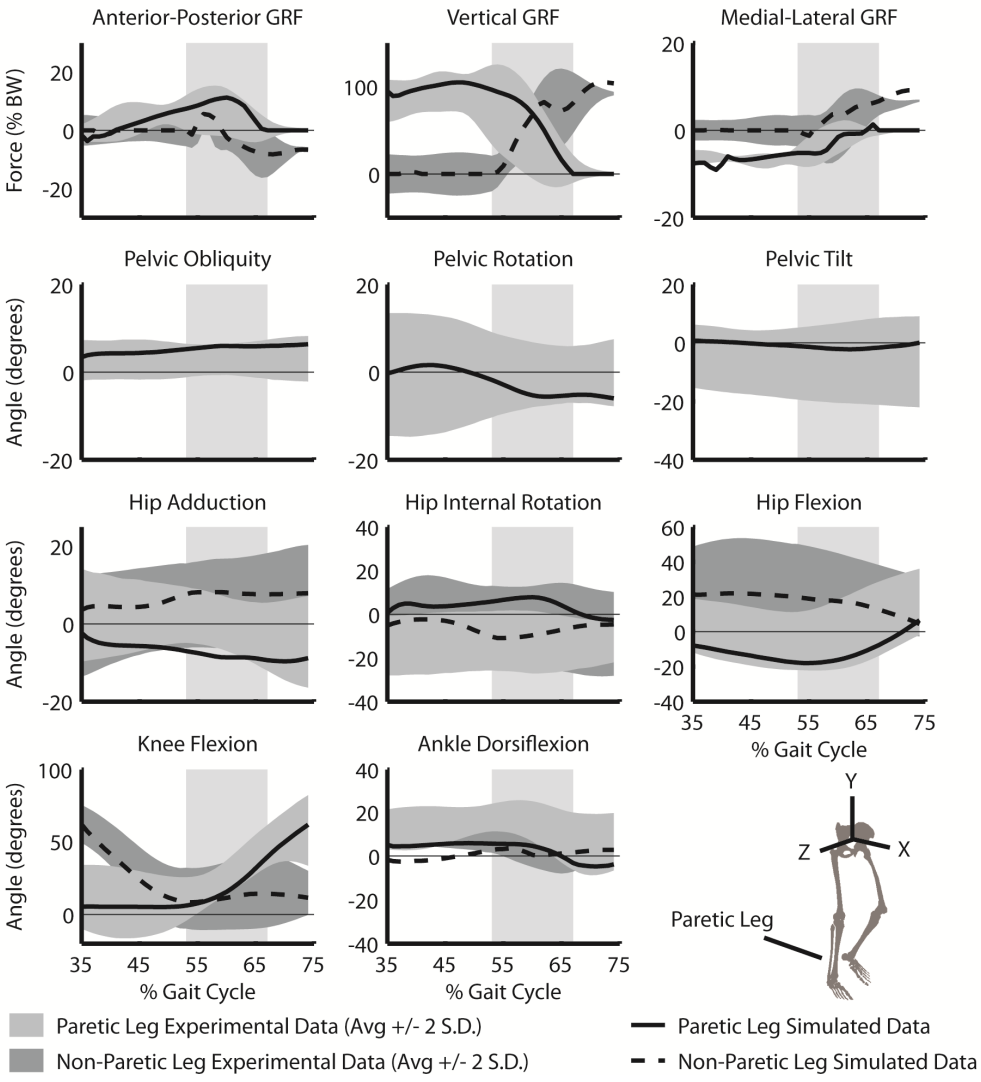

Figure D3. Simulated and experimental ground reaction force (GRF) and kinematic data for the community hemiparetic walkers who were included in the study in Chapter 2. Experimental data are normalized to the paretic leg gait cycle and shown as the average +/- 2 standard deviations (S.D.). Positive joint angles correspond to plot subtitles. Positive pelvic obliquity, rotation and tilt correspond to positive rotations about the X, Y and Z pelvis segment axes, respectively (see bottom right). The shaded vertical bar indicates the paretic leg pre-swing region.

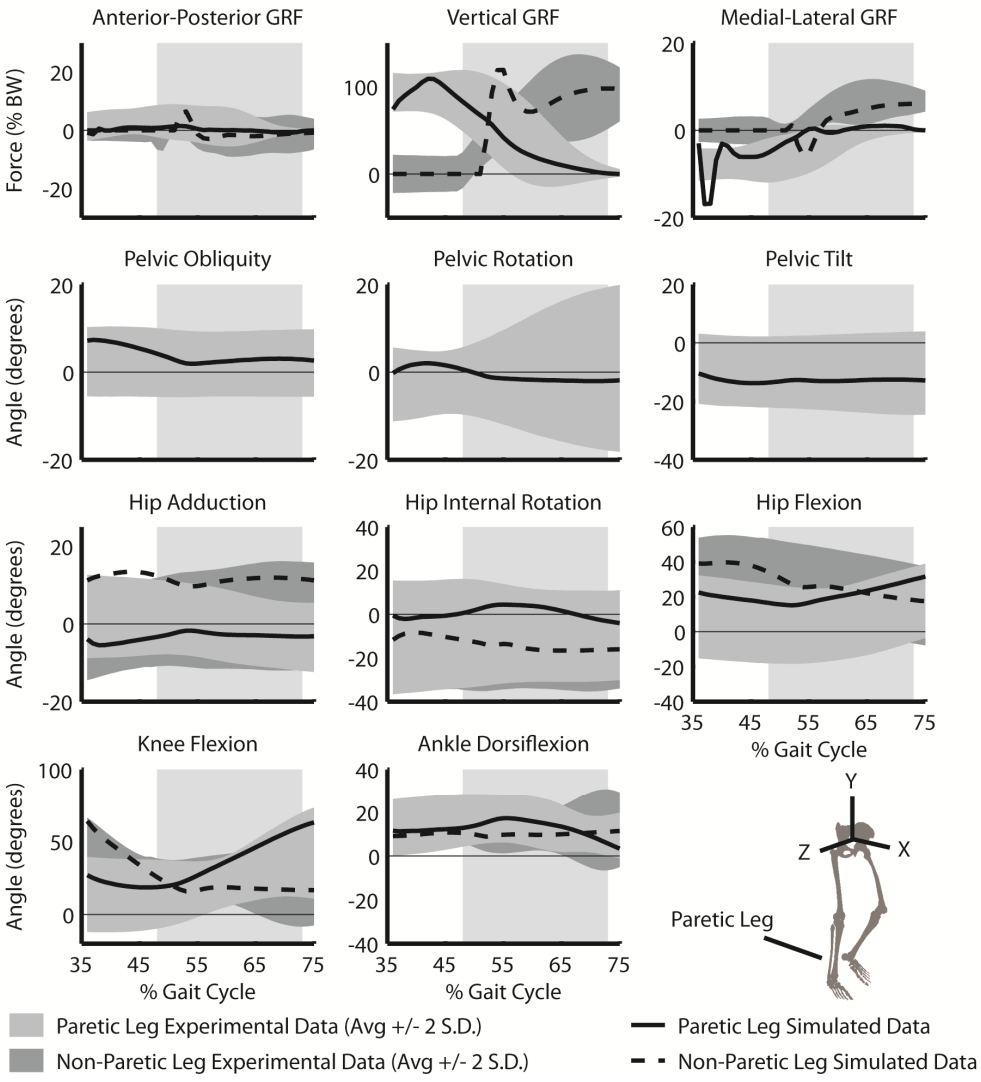

Figure D4. Simulated and experimental ground reaction force (GRF) and kinematic data for the limited community hemiparetic walkers who were included in the study in Chapter 2. Experimental data are normalized to the paretic leg gait cycle and shown as the average +/- 2 standard deviations (S.D.). Positive joint angles correspond to plot subtitles. Positive pelvic obliquity, rotation and tilt correspond to positive rotations about the X, Y and Z pelvis segment axes, respectively (see bottom right). The shaded vertical bar indicates the paretic leg pre-swing region.

References

Ada, L., Dean, C.M., Hall, J.M., Bampton, J. and Crompton, S., (2003). A treadmill and overground walking program improves walking in persons residing in the community after stroke: A placebo-controlled, randomized trial. *Arch Phys Med Rehabil* 84 (10), 1486-1491.

Allen, J.L., Kautz, S.A. and Neptune, R.R., (2010). Step length asymmetry is representative of compensatory mechanisms used in post-stroke hemiparetic walking. *Gait Posture* (in review).

Anderson, F.C. and Pandy, M.G., (1999). A dynamic optimization solution for vertical jumping in three dimensions. *Comput Methods Biomech Biomed Engin* 2 (3), 201-231.

Anderson, F.C., 1999. A dynamic optimization solution for a complete cycle of normal gait. Doctoral Dissertation, The University of Texas at Austin, Austin, TX.

Anderson, F.C. and Pandy, M.G., (2001). Dynamic optimization of human walking. *J Biomech Eng* 123 (5), 381-390.

Balasubramanian, C.K., Bowden, M.G., Neptune, R.R. and Kautz, S.A., (2007). Relationship between step length asymmetry and walking performance in subjects with chronic hemiparesis. *Arch Phys Med Rehabil* 88 (1), 43-49.

Barbeau, H. and Visintin, M., (2003). Optimal outcomes obtained with body-weight support combined with treadmill training in stroke subjects. *Arch Phys Med Rehabil* 84 (10), 1458-1465.

Bohannon, R.W., Andrews, A.W. and Smith, M.B., (1988). Rehabilitation goals of patients with hemiplegia. *Int J Rehabil Res* 11 (2), 181-184.

Bowden, M.G., Balasubramanian, C.K., Neptune, R.R. and Kautz, S.A., (2006). Anterior-posterior ground reaction forces as a measure of paretic leg contribution in hemiparetic walking. *Stroke* 37 (3), 872-876.

Bowden, M.G., Balasubramanian, C.K., Behrman, A.L. and Kautz, S.A., (2008). Validation of a speed-based classification system using quantitative measures of walking performance poststroke. *Neurorehabil Neural Repair* 22 (6), 672-675.

Chen, G. and Patten, C., (2008). Joint moment work during the stance-to-swing transition in hemiparetic subjects. *J Biomech* 41 (4), 877-883.

Davy, D.T. and Audu, M.L., (1987). A dynamic optimization technique for predicting muscle forces in the swing phase of gait. *J Biomech* 20 (2), 187-201.

De Quervain, I.A., Simon, S.R., Leurgans, S., Pease, W.S. and McAllister, D., (1996). Gait pattern in the early recovery period after stroke. *J Bone Joint Surg Am* 78 (10), 1506-1514.

Delp, S.L., Loan, J.P., Hoy, M.G., Zajac, F.E., Topp, E.L. and Rosen, J.M., (1990). An interactive graphics-based model of the lower extremity to study orthopaedic surgical procedures. *IEEE Trans Biomed Eng* 37 (8), 757-767.

Delp, S.L., Anderson, F.C., Arnold, A.S., Loan, P., Habib, A., John, C.T., Guendelman, E. and Thelen, D.G., (2007). Opensim: Open-source software to create and analyze dynamic simulations of movement. *IEEE Trans Biomed Eng* 54 (11), 1940-1950.

den Otter, A.R., Geurts, A.C., Mulder, T. and Duysens, J., (2004). Speed related changes in muscle activity from normal to very slow walking speeds. *Gait Posture* 19 (3), 270-278.

den Otter, A.R., Geurts, A.C., Mulder, T. and Duysens, J., (2007). Abnormalities in the temporal patterning of lower extremity muscle activity in hemiparetic gait. *Gait Posture* 25 (3), 342-352.

Fregly, B.J. and Zajac, F.E., (1996). A state-space analysis of mechanical energy generation, absorption, and transfer during pedaling. *J Biomech* 29 (1), 81-90.

Gao, F., Grant, T.H., Roth, E.J. and Zhang, L.Q., (2009). Changes in passive mechanical properties of the gastrocnemius muscle at the muscle fascicle and joint levels in stroke survivors. *Arch Phys Med Rehabil* 90 (5), 819-826.

Goffe, W.L., Ferrier, G.D. and Rogers, J., (1994). Global optimization of statistical functions with simulated annealing. *J Econometrics* 60 (1-2), 65-99.

Hall, A.L., Peterson, C.L., Kautz, S.A. and Neptune, R.R., (2010). Relationships between muscle contributions to walking subtasks and functional walking status in persons with post-stroke hemiparesis. *Clin Biomech* (in review).

Harris, J.E. and Eng, J.J., (2004). Goal priorities identified through client-centred measurement in individuals with chronic stroke. *Physiother Can* 56 (03), 171+.

Hesse, S., Bertelt, C., Jahnke, M.T., Schaffrin, A., Baake, P., Malezic, M. and Mauritz, K.H., (1995). Treadmill training with partial body weight support compared with physiotherapy in nonambulatory hemiparetic patients. *Stroke* 26 (6), 976-981.

Higginson, J.S., Zajac, F.E., Neptune, R.R., Kautz, S.A. and Delp, S.L., (2006). Muscle contributions to support during gait in an individual with post-stroke hemiparesis. *J Biomech* 39 (10), 1769-1777.

Kelly-Hayes, M., Beiser, A., Kase, C.S., Scaramucci, A., D'Agostino, R.B. and Wolf, P.A., (2003). The influence of gender and age on disability following ischemic stroke: The Framingham study. *J Stroke Cerebrovasc Dis* 12 (3), 119-126.

Kepple, T.M., Siegel, K.L. and Stanhope, S.J., (1997). Relative contributions of the lower extremity joint moments to forward progression and support during gait. *Gait Posture* 6 (1), 1-8.

Liu, M.Q., Anderson, F.C., Pandy, M.G. and Delp, S.L., (2006). Muscles that support the body also modulate forward progression during walking. *J Biomech* 39 (14), 2623-2630.

Liu, M.Q., Anderson, F.C., Schwartz, M.H. and Delp, S.L., (2008). Muscle contributions to support and progression over a range of walking speeds. *J Biomech* 41 (15), 3243-3252.

Lloyd-Jones, D., Adams, R.J., Brown, T.M., Carnethon, M., Dai, S., De Simone, G., Ferguson, T.B., Ford, E., Furie, K., Gillespie, C., Go, A., Greenlund, K., Haase, N., Hailpern, S., Ho, P.M., Howard, V., Kissela, B., Kittner, S., Lackland, D., Lisabeth, L., Marelli, A., McDermott, M.M., Meigs, J., Mozaffarian, D., Mussolino, M., Nichol, G., Roger, V.L., Rosamond, W., Sacco, R., Sorlie, P., Stafford, R., Thom, T., Wasserthiel-Smoller, S., Wong, N.D. and Wylie-Rosett, J., (2010). Heart disease and stroke statistics-2010 update: A report from the american heart association. *Circulation* 121 (7), e46-e215.

Macko, R.F., Haeuber, E., Shaughnessy, M., Coleman, K.L., Boone, D.A., Smith, G.V. and Silver, K.H., (2002). Microprocessor-based ambulatory activity monitoring in stroke patients. *Med Sci Sports Exerc* 34 (3), 394-399.

McGowan, C.P., Neptune, R.R. and Kram, R., (2008). Independent effects of weight and mass on plantar flexor activity during walking: Implications for their contributions to body support and forward propulsion. *J Appl Physiol* 105 (2), 486-494.

Menegaldo, L.L., de Toledo Fleury, A. and Weber, H.I., (2004). Moment arms and musculotendon lengths estimation for a three-dimensional lower-limb model. *J Biomech* 37 (9), 1447-1453.

Mulroy, S.J., Klassen, T., Gronley, J.K., Eberly, V.J., Brown, D.A. and Sullivan, K.J., (2010). Gait parameters associated with responsiveness to treadmill training with body-weight support after stroke: An exploratory study. *Phys Ther* 90 (2), 209-223.

Nadeau, S., Gravel, D., Arsenault, A.B. and Bourbonnais, D., (1999). Plantarflexor weakness as a limiting factor of gait speed in stroke subjects and the compensating role of hip flexors. *Clin Biomech* 14 (2), 125-135.

Neptune, R.R., Wright, I.C. and Van Den Bogert, A.J., (2000). A method for numerical simulation of single limb ground contact events: Application to heel-toe running. *Comput Methods Biomech Biomed Engin* 3 (4), 321-334.

Neptune, R.R., Kautz, S.A. and Zajac, F.E., (2001). Contributions of the individual ankle plantar flexors to support, forward progression and swing initiation during walking. *J Biomech* 34 (11), 1387-1398.

Neptune, R.R., Zajac, F.E. and Kautz, S.A., (2004). Muscle force redistributes segmental power for body progression during walking. *Gait Posture* 19 (2), 194-205.

Neptune, R.R., Sasaki, K. and Kautz, S.A., (2008). The effect of walking speed on muscle function and mechanical energetics. *Gait Posture* 28 (1), 135-143.

Nott, C.R., Zajac, F.E., Neptune, R.R. and Kautz, S.A., (2010). Abnormalities in pre-swing phase during hemiparetic walking. *Gait Posture* (in review).

Olney, S.J., Griffin, M.P., Monga, T.N. and McBride, I.D., (1991). Work and power in gait of stroke patients. *Arch Phys Med Rehabil* 72 (5), 309-314.

Olney, S.J. and Richards, C., (1996). Hemiparetic gait following stroke. Part I: Characteristics. *Gait Posture* 4 (2), 136-148.

Parvataneni, K., Olney, S.J. and Brouwer, B., (2007). Changes in muscle group work associated with changes in gait speed of persons with stroke. *Clin Biomech* 22 (7), 813-820.

Patterson, K.K., Gage, W.H., Brooks, D., Black, S.E. and McIlroy, W.E., (2010). Evaluation of gait symmetry after stroke: A comparison of current methods and recommendations for standardization. *Gait Posture* 31 (2), 241-246.

Perry, J., Garrett, M., Gronley, J.K. and Mulroy, S.J., (1995). Classification of walking handicap in the stroke population. *Stroke* 26 (6), 982-989.

Peterson, C.L., Cheng, J., Kautz, S.A. and Neptune, R.R., (2010). Leg extension is an important predictor of paretic leg propulsion in hemiparetic walking. *Gait Posture* 32 (4), 451-456.

Peterson, C.L., Hall, A.L., Kautz, S.A. and Neptune, R.R., (2010). Pre-swing deficits in forward propulsion, swing initiation and power generation by individual muscles during hemiparetic walking. *J Biomech* 43 (12), 2348-2355.

Peurala, S.H., Tarkka, I.M., Pitkanen, K. and Sivenius, J., (2005). The effectiveness of body weight-supported gait training and floor walking in patients with chronic stroke. *Arch Phys Med Rehabil* 86 (8), 1557-1564.

Plummer, P., Behrman, A.L., Duncan, P.W., Spigel, P., Saracino, D., Martin, J., Fox, E., Thigpen, M. and Kautz, S.A., (2007). Effects of stroke severity and training duration on locomotor recovery after stroke: A pilot study. *Neurorehabil Neural Repair* 21 (2), 137-151.

Raasch, C.C., Zajac, F.E., Ma, B. and Levine, W.S., (1997). Muscle coordination of maximum-speed pedaling. *J Biomech* 30 (6), 595-602.

Sullivan, K.J., Brown, D.A., Klassen, T., Mulroy, S., Ge, T., Azen, S.P., Winstein, C.J. and, (2007). Effects of task-specific locomotor and strength training in adults who were ambulatory after stroke: Results of the steps randomized clinical trial. *Phys Ther* 87 (12), 1580-1602.

Sutherland, D.H. (1984). Gait disorders in childhood and adolescence. Baltimore, MD, Williams and Wilkins.

Teixeira-Salmela, L.F., Nadeau, S., Mcbride, I. and Olney, S.J., (2001). Effects of muscle strengthening and physical conditioning training on temporal, kinematic and kinetic variables during gait in chronic stroke survivors. *J Rehabil Med* 33 (2), 53-60.

Thelen, D.G., Anderson, F.C. and Delp, S.L., (2003). Generating dynamic simulations of movement using computed muscle control. *J Biomech* 36 (3), 321-328.

Thelen, D.G. and Anderson, F.C., (2006). Using computed muscle control to generate forward dynamic simulations of human walking from experimental data. *J Biomech* 39 (6), 1107-1115.

Tilson, J.K., Sullivan, K.J., Cen, S.Y., Rose, D.K., Koradia, C.H., Azen, S.P. and Duncan, P.W., (2010). Meaningful gait speed improvement during the first 60 days poststroke: Minimal clinically important difference. *Phys Ther* 90 (2), 196-208.

Turns, L.J., Neptune, R.R. and Kautz, S.A., (2007). Relationships between muscle activity and anteroposterior ground reaction forces in hemiparetic walking. *Arch Phys Med Rehabil* 88 (9), 1127-1135.

Visintin, M., Barbeau, H., Korner-Bitensky, N. and Mayo, N.E., (1998). A new approach to retrain gait in stroke patients through body weight support and treadmill stimulation. *Stroke* 29 (6), 1122-1128.

Winters, J.M. and Stark, L., (1988). Estimated mechanical properties of synergistic muscles involved in movements of a variety of human joints. *J Biomech* 21 (12), 1027-1041.

Yamaguchi, G.T. and Zajac, F.E., (1989). A planar model of the knee joint to characterize the knee extensor mechanism. *J Biomech* 22 (1), 1-10.

Yates, J.S., Studenski, S., Gollub, S., Whitman, R., Perera, S., Min, S. and Duncan, P.W., (2004). Bicycle ergometry in subacute-stroke survivors: Feasibility, safety, and exercise performance. *J Aging Phys Act* 12 (1), 64-74.

Zajac, F.E., (1989). Muscle and tendon: Properties, models, scaling, and application to biomechanics and motor control. *Crit Rev Biomed Eng* 17 (4), 359-411.

Vita

Allison Leigh Hall was born in Galveston, TX and grew up in League City, TX. Allison attended Clear Creek High School in League City, TX and graduated in 2001. After high school graduation, she began undergraduate studies at Tulane University where she majored in Biomedical Engineering and earned a Bachelor of Science degree in May 2005. In the summers of 2003 and 2004, Allison participated in a summer research program in the Department of Orthopaedic Surgery at The University of Texas Health Science Center in Houston, TX. In August of 2005, Allison began graduate studies in Mechanical Engineering at The University of Texas at Austin in the Neuromuscular Biomechanics Laboratory. She graduated in August 2007 with a Master of Science in Engineering from The University of Texas at Austin. Allison continued her graduate studies at The University of Texas at Austin and her research has focused on using simulation and experimental analyses to investigate post-stroke hemiparetic walking.

Permanent email address: allison.l.hall@gmail.com

This dissertation was typed by the author.